

# F<sup>2</sup>RVLM: Boosting Fine-grained Fragment Retrieval for Multi-Modal Long-form Dialogue with Vision Language Model

Hanbo Bi\*, Zhiqiang Yuan\*, Zexi Jia, Jiapei Zhang, Chongyang Li,  
Peixiang Luo, Ying Deng, Xiaoyue Duan, Jinchao Zhang<sup>†</sup>

Pattern Recognition Center, WeChat AI, Tencent Inc, China

## Abstract

Traditional dialogue retrieval aims to select the most appropriate utterance or image from recent dialogue history. However, they often fail to meet users' actual needs for revisiting semantically coherent content scattered across long-form conversations. To fill this gap, we define the Fine-grained Fragment Retrieval (FFR) task, requiring models to locate query-relevant fragments, comprising both utterances and images, from multimodal long-form dialogues. As a foundation for FFR, we construct MLDR, the longest-turn multimodal dialogue retrieval dataset to date, averaging 25.45 turns per dialogue, with each naturally spanning three distinct topics. To evaluate generalization in real-world scenarios, we curate and annotate a WeChat-based test set comprising real-world multimodal dialogues with an average of 75.38 turns. Building on these resources, we explore existing generation-based Vision-Language Models (VLMs) on FFR and observe that they often retrieve incoherent utterance-image fragments. While optimized for generating responses from visual-textual inputs, these models lack explicit supervision to ensure semantic coherence within retrieved fragments. To address this, we propose F<sup>2</sup>RVLM, a generative retrieval model trained in a two-stage paradigm: (1) supervised fine-tuning to inject fragment-level retrieval knowledge, and (2) GRPO-based reinforcement learning with multi-objective rewards to encourage outputs with semantic precision, relevance, and contextual coherence. In addition, to account for difficulty variations arising from differences in intra-fragment element distribution, ranging from locally dense to sparsely scattered, we introduce a difficulty-aware curriculum sampling that ranks training instances by predicted difficulty and gradually incorporates harder examples. This strategy enhances the model's reasoning ability in long, multi-turn dialogue contexts. Experiments on both in-domain and real-domain sets demonstrate that F<sup>2</sup>RVLM substantially outperforms popular VLMs, achieving superior retrieval performance. Code and dataset are available at <https://f2rvlm.github.io>.

## Introduction

With the widespread adoption of messaging platforms and AI assistants, users frequently need to revisit earlier utterances or referenced images for information confirmation or context tracking. Efficiently retrieving specific content

\*These authors contributed equally.

<sup>†</sup>Corresponding author: Jinchao Zhang

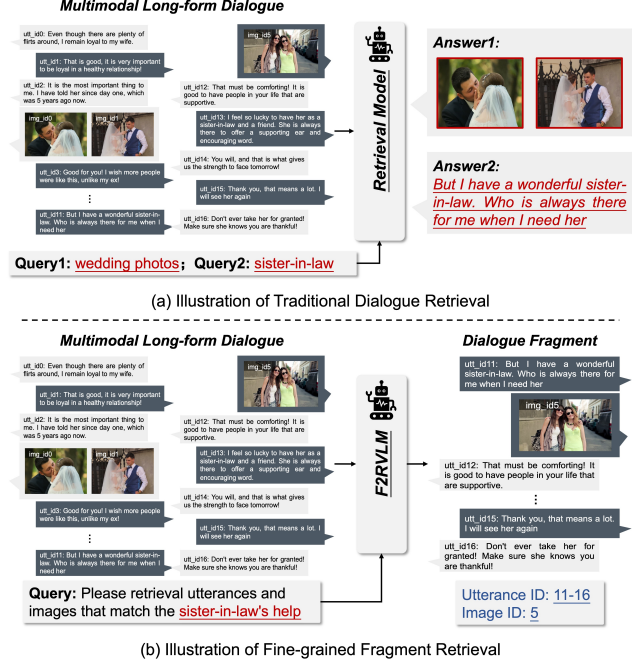


Figure 1: Comparison between the traditional Dialogue Retrieval and our Fine-grained Fragment Retrieval task.

from ongoing multimodal dialogues has become a crucial capability for intelligent systems. Such dialogues often span dozens of turns, intertwining multiple topics, user intents, and visual-textual cues. As illustrated in Fig.1, unlike conventional retrieval tasks that select the most appropriate element from the dialogue history, this scenario demands models to directly locate semantically coherent fragments, including both text and images, enabling users to efficiently access relevant historical content. To address this need, we define the **Fine-grained Fragment Retrieval (FFR)** task, which aims to accurately extract query-relevant fragments from long-form, multi-party, multimodal dialogues.

As a foundation for studying FFR, we construct MLDR, a large-scale multimodal long-form dialogue retrieval dataset. Each dialogue covers three distinct topics with an average of 25.45 turns, making it the longest-turn multimodal dialogue dataset to date. To support diverse retrieval intents, we provide multi-granularity annotations, including domain-level

and event-level tags for each dialogue unit. In addition, we curate a WeChat-based test set comprising real-world multimodal dialogues with an average of 75.38 turns, aiming to evaluate generalization in practical settings. This set is collected from real conversations contributed by multiple volunteers and annotated through a multi-stage process, serving as a realistic and challenging benchmark for fragment retrieval (see Appendix.A for details).

Building on our constructed dataset resources, we investigate existing retrieval models on the proposed FFR task. In retrieval scenarios, current models predominantly follow two paradigms: embedding-based and generation-based. Embedding-based Vision-Language Models (VLMs), such as CLIP (Radford et al. 2021) and BLIP2 (Li et al. 2023), encode images and texts into a shared embedding space and retrieve via similarity ranking. In contrast, generation-based models are typically pre-trained on large-scale image-text corpora to align cross-modal semantics, and subsequently instruction-tuned to generate responses conditioned on visual-textual inputs. Models like GPT-4o (Jaech et al. 2024) and Gemini (Comanici et al. 2025) demonstrate strong performance in prompt-driven retrieval settings, leveraging unified architectures with promising contextual understanding in open-ended multimodal dialogues.

Despite their general success, our evaluation reveals that even leading VLMs struggle to localize relevant fragments accurately in long-form multimodal dialogues. Models such as Qwen2.5-VL-72B (Wang et al. 2024) and Doubao-Seed-1.6 (Guo et al. 2025a) frequently retrieve incoherent utterance-image pairs, e.g., mismatched dialogue turns or irrelevant visual content, resulting in suboptimal F1 scores under real-world conditions (see qualitative examples in Appendix.C). This limitation primarily stems from the gap between the models’ learning objectives and the demands of fragment retrieval: while optimized for generating responses from visual-textual inputs, these models lack explicit supervision to ensure that the retrieved or generated fragments (both utterances and images) are semantically coherent and contextually aligned with the user query.

To address these limitations, we propose **F<sup>2</sup>RVLM**, a generation-based retrieval framework for long-form multimodal dialogues, tailored for **Fine-grained Fragment Retrieval with Vision-Language Model**. F<sup>2</sup>RVLM follows a two-stage training paradigm: fragment-level retrieval knowledge is first injected via supervised fine-tuning, followed by GRPO-based reinforcement learning to align retrieval behavior with human preferences. We design a multi-objective reward scheme that encourages the generation of fragments with semantic precision and contextual coherence. Specifically: (1) an F1-based alignment reward encourages accurate matching with ground-truth fragments, penalizing both over- and under-retrieval; (2) a fragment order consistency enhances semantic alignment between selected utterances and images, guiding the model to organize content in a coherent, human-preferred manner. Moreover, we observe that fragment structures in long-form dialogues differ in their internal distribution, from locally dense to sparsely scattered, which directly reflects differences in retrieval difficulty. To exploit this inherent hierarchy of difficulty, we in-

duce a curriculum sampling that ranks training samples by predicted F1 and confidence, progressively exposing the model to harder instances with greater contextual complexity. This promotes robust reasoning in diverse, noisy, and long-range scenarios. Extensive experiments on both the in-domain MLDR and real-domain WeChat-based sets demonstrate that F<sup>2</sup>RVLM significantly outperforms mainstream VLMs in retrieval accuracy and contextual understanding.

Our main contributions are summarized as follows:

- We introduce Fine-grained Fragment Retrieval, a novel retrieval task that aims to directly locate semantically coherent utterance-image fragments from long-form dialogues, differing from traditional dialogue retrieval that selects the most appropriate individual elements.
- We construct MLDR, the longest-turn multimodal dialogue retrieval dataset to date, averaging 25.45 turns per dialogue, with each covering three distinct topics. Additionally, we curate a real-world WeChat-based test set averaging 75.38 turns per dialogue to evaluate retrieval generalization in practice.
- We propose F<sup>2</sup>RVLM, a generation-based retrieval model for the proposed task. It integrates GRPO-based reinforcement learning with multi-objective rewards and difficulty-aware curriculum sampling to progressively enhance the semantic consistency and completeness of retrieved fragments.
- Experimental results on both the in-domain MLDR validation set and the real-domain WeChat-based test set demonstrate that F<sup>2</sup>RVLM consistently outperforms popular VLMs in fragment retrieval accuracy.

## Related Work

**Multimodal Dialogue Datasets.** Recent advances in vision-language modeling have accelerated progress in multimodal dialogue understanding (Meng et al. 2020). Existing dialogue datasets fall into two main types: (1) Image-grounded datasets (Shuster et al. 2020; Zheng et al. 2022; Lin et al. 2023) consist of dialogues explicitly constructed around a given image, often collected via crowdsourcing. While well-aligned, they lack the natural heterogeneity of real conversations, where not all utterances refer to images. (2) Image-sharing datasets (Zang et al. 2021; Lee et al. 2021; Feng et al. 2023; Lee et al. 2024) address this by capturing more spontaneous visual usage. For instance, MMDialog (Feng et al. 2023) collects over 1M social media conversations with images dispersed across turns, while DialogCC (Lee et al. 2024) enriches textual dialogues by inserting suitable images. However, these corpora still consist mostly of short, single-topic dialogues and lack the long-range, multi-topic structure of real-world interactions.

**VLMs for Dialogue Retrieval.** VLMs have achieved notable success in image-text retrieval, typically following two paradigms: (1) embedding-based VLMs (Radford et al. 2021; Li et al. 2022; Liu et al. 2022; Zhang et al. 2024; Wei et al. 2024a) that learn joint visual-text representations for efficient matching, and (2) generation-based VLMs (Liu et al. 2023a; Achiam et al. 2023; Wang et al. 2024; Jiang

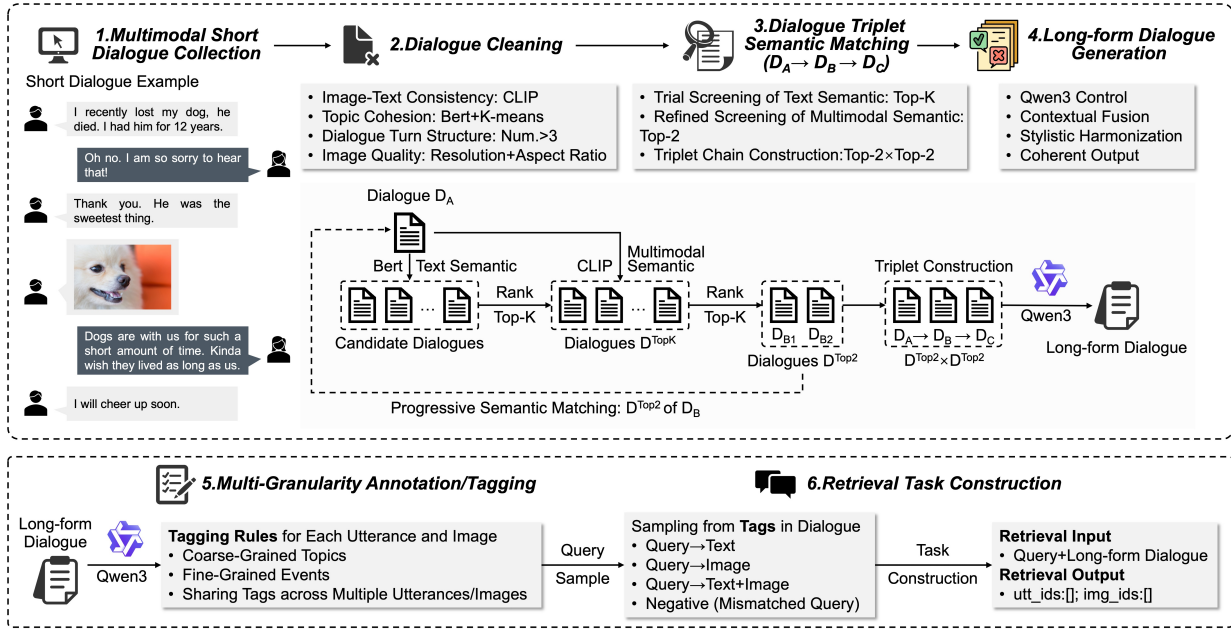


Figure 2: Overview of the MLDR construction pipeline, which integrates multimodal short dialogue processing, Qwen3-driven long-form dialogue generation, multi-granularity annotation, and retrieval-oriented task design.

et al. 2024b; Liu et al. 2025a) that combine LLMs with visual encoders to generate context-aware responses via multimodal prompts. Recently, multimodal dialogue retrieval has gained traction, focusing on selecting the most appropriate sentence or image given the dialogue history (Yin et al. 2024; Choe, Oh, and Yang 2025). For example, DRIBER (Lee et al. 2023) and VCU (Wei et al. 2024b) generate intermediate image descriptions for dialogue-to-image retrieval, while IGSR (Wang et al. 2025a) retrieves stickers by identifying user intent. However, these tasks are constrained to short-context response selection. In this work, we investigate a more challenging yet underexplored setting, Fine-grained Fragment Retrieval, which aims to retrieve semantically aligned fragments scattered across long-form, multi-topic dialogues.

**VLMs with Reinforcement Learning.** Recent advances like OpenAI’s o1 (Jaech et al. 2024) and DeepSeek-R1 (Guo et al. 2025b) have shifted LLM research toward enhancing reasoning via reinforcement learning (RL), leading to paradigms such as GRPO (Shao et al. 2024), DAPO (Yu et al. 2025), and VAPO (Yue et al. 2025). This trend is expanding into the multimodal domain (Shen et al. 2025; Wang et al. 2025b), with methods like LMM-R1 (Peng et al. 2025) introducing rule-based two-stage RL, and Reason-RFT (Tan et al. 2025) using SFT with CoT data for RL initialization. Vision-R1 (Huang et al. 2025) employs progressive reflection suppression in GRPO, while Visual-RFT (Liu et al. 2025b) enhances visual reasoning via verifiable rewards. Video-R1 (Feng et al. 2025) further extends GRPO with temporal modeling for video-language tasks. In this work, we explore RL for multimodal dialogue content retrieval, aiming to improve fine-grained reasoning and fragment localization in long-form image-text contexts.

#	Datasets	Avg. Turn	Avg. Topic
ENG	ImageChat (Shuster et al. 2020)	1.98	1.00
	OpenViDial (Meng et al. 2020)	1.00	1.00
	PhotoChat (Zang et al. 2021)	12.74	1.00
	MMDD (Lee et al. 2021)	11.56	1.00
	MMDialog (Feng et al. 2023)	4.56	1.00
	DialogCC (Lee et al. 2024)	8.20	1.00
CN	MMChat (Zheng et al. 2022)	2.59	1.00
	M3ED (Zhao et al. 2022)	9.17	1.00
	CPED (Chen et al. 2022)	11.08	1.00
	CMMA (Zhang et al. 2023)	7.27	1.00
	TikTalk (Lin et al. 2023)	2.25	1.00
	<b>Our MLDR Dataset</b>	<b>25.45</b>	<b>3.00</b>

Table 1: Summary of main multimodal dialogue datasets.

## MLDR Dataset

This section outlines the construction of MLDR and the WeChat test set, along with their statistical analysis.

## MLDR Construction

As highlighted in Table 1, existing multimodal dialogue datasets primarily consist of short, single-topic conversations, limiting their utility in modeling the multi-topic nature of real-world dialogues. To fill this gap, we construct a multimodal long-form dialogue corpus and further develop the MLDR dataset. The pipeline is illustrated in Fig.2 and summarized below (see Appendix.A for details):

**Short Dialogue Collection & Cleaning.** We begin with topic-rich short dialogues from DialogCC, providing a semantically diverse foundation for coherent long-form generation. To ensure data quality, we apply a multi-criteria cleaning pipeline to remove samples with poor image-text alignment, topic drift, unstructured turns, or low image quality.

**Dialogue Triplet Semantic Matching.** To construct coherent long-form dialogues, we design a triplet-based matching strategy that ensures topic continuity and multimodal alignment. For each short dialogue  $D_A$ , we first identify the Top-

$K$  semantically similar candidates using BERT-based sentence embeddings. We then refine this set by computing a weighted multimodal similarity score with CLIP (0.7 for text, 0.3 for image), and select the Top-2 most aligned dialogues  $D_B$ . This process is repeated for each  $D_B$  to retrieve two additional candidates  $D_C$ , forming four unique triplets of the form  $D_A \rightarrow D_B \rightarrow D_C$ , which serve as structural units for long-form synthesis.

**Long-form Dialogue Generation.** Each matched triplet is converted into a coherent long-form dialogue utilizing the Qwen3-256B (Yang et al. 2025) model with structured prompts. The generation process preserves multimodal semantics, ensures topical coherence through smooth transitions, and yields fluent, contextually grounded long-form dialogues, forming high-quality samples for downstream retrieval and reasoning tasks.

**Multi-Granularity Annotation.** To support fine-grained fragment retrieval, we adopt a two-level shared tagging scheme automatically generated by the Qwen3 under structured prompts. Each sentence and image caption is assigned a coarse-grained tag (e.g., domain) and a fine-grained tag (e.g., event), with each tag shared by at least two elements to form semantically consistent fragments.

**Task Construction for Retrieval.** We formulate a unified retrieval task over annotated long-form dialogues, where sampled coarse- or fine-grained tags serve as natural language queries, and corresponding utterances/images sharing the same tag form the retrieval fragments. To enhance diversity and robustness, we adopt a query-driven sampling strategy that generates four types of query-fragment pairs: (a) multimodal fragments; (b) utterance-only fragments; (c) image-only fragments; and (d) negative samples constructed by replacing queries with unrelated tags. This formulation supports generalization across varied retrieval scenarios.

## Real-domain Evaluation on WeChat Dialogues

To evaluate fine-grained retrieval in real-world scenarios, we construct a real-domain test set from naturally occurring multimodal WeChat conversations. Unlike the synthesized MLDR data, these dialogues reflect authentic user interactions, with noisy inputs, informal expressions, and frequent topic shifts, posing greater challenges for robust retrieval.

We collect multi-turn image-utterance chats from 12 volunteers<sup>1</sup> and preprocess them by removing emojis, sensitive content, profanity, and semantically void utterances. Consecutive messages from the same speaker are merged, and only dialogues with at least two images are retained. This yields 270 long-form dialogues (avg. 145.38 turns), which are segmented if exceeding 100 turns, resulting in 580 coherent samples. All dialogues are manually annotated by a professionally trained team, producing 1,250 query-dialogue pairs. Each sample includes a natural language query, its multimodal dialogue (avg. 75.38 turns), and ground-truth utterance and image IDs as retrieval targets. The task format

<sup>1</sup>Volunteers manually provided their own chat records from the application. We emphasize that all data were solely provided by volunteers, and no chat records were, or will ever be, obtained from WeChat’s backend.

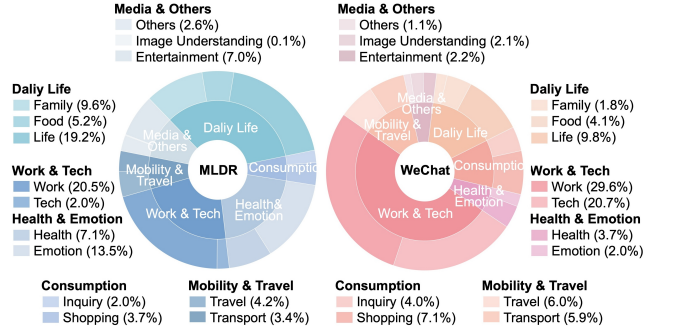


Figure 3: Comparison between the MLDR and WeChat-based datasets in terms of dialogue topic distributions.

remains consistent with MLDR, enabling direct evaluation of model generalization in open-domain fragment retrieval.

## Dataset Statistics and Analysis

To better understand the characteristics of MLDR and its real-world generalization benchmark, we compare topic diversity between MLDR and the WeChat-based test set (Fig.3). We organize dialogue content into six high-level domains (e.g., Daily Life, Work & Tech), further divided into 14 fine-grained topics. Each MLDR dialogue is deliberately constructed to span three distinct topics, promoting multi-topic contextual modeling and ensuring a balanced semantic distribution. In contrast, the WeChat-based test set exhibits natural domain bias, with over 50% of conversations centered on Work & Tech. Further comparisons of dialogue turn distributions are provided in the Appendix.A.

## Methodology

### Task Definition

Fine-grained fragment retrieval (FFR) can be formulated as a structured prediction task over long-form, multi-turn dialogues that include both textual utterances and images. Given a multimodal dialogue  $D = \{(u_1, m_1), (u_2, m_2), \dots, (u_T, m_T)\}$ , where each turn  $t$  consists of a speaker  $u_t$  and a message  $m_t$  that may contain text or images, and a user-issued query  $q$ , the objective is to retrieve a subset of utterance and image IDs that are semantically relevant to the query. To enable the VLMs to perceive and understand the semantic and temporal structure of each turn, explicit structural markers are inserted into the dialogue:  $<|utt\_id\_start|> \dots <|utt\_id\_end|>$  to mark each utterance with a unique ID, while  $<|img\_id\_start|> \dots <|img\_id\_end|>$  marks each embedded image. In summary, the retrieval process can be formalized as:

$$\hat{y} = \mathcal{F}(D, q) = (\hat{I}_{\text{utt}}, \hat{I}_{\text{img}}) \quad (1)$$

where  $\hat{I}_{\text{utt}}$  and  $\hat{I}_{\text{img}}$  denote the predicted sets of relevant utterance and image IDs, respectively.

### Framework Overview

As illustrated in Fig.4, given a long-form dialogue  $D$  and a query  $q$ , F<sup>2</sup>RVLML generates structured outputs of relevant utterance and image IDs. To enable this behavior, the model

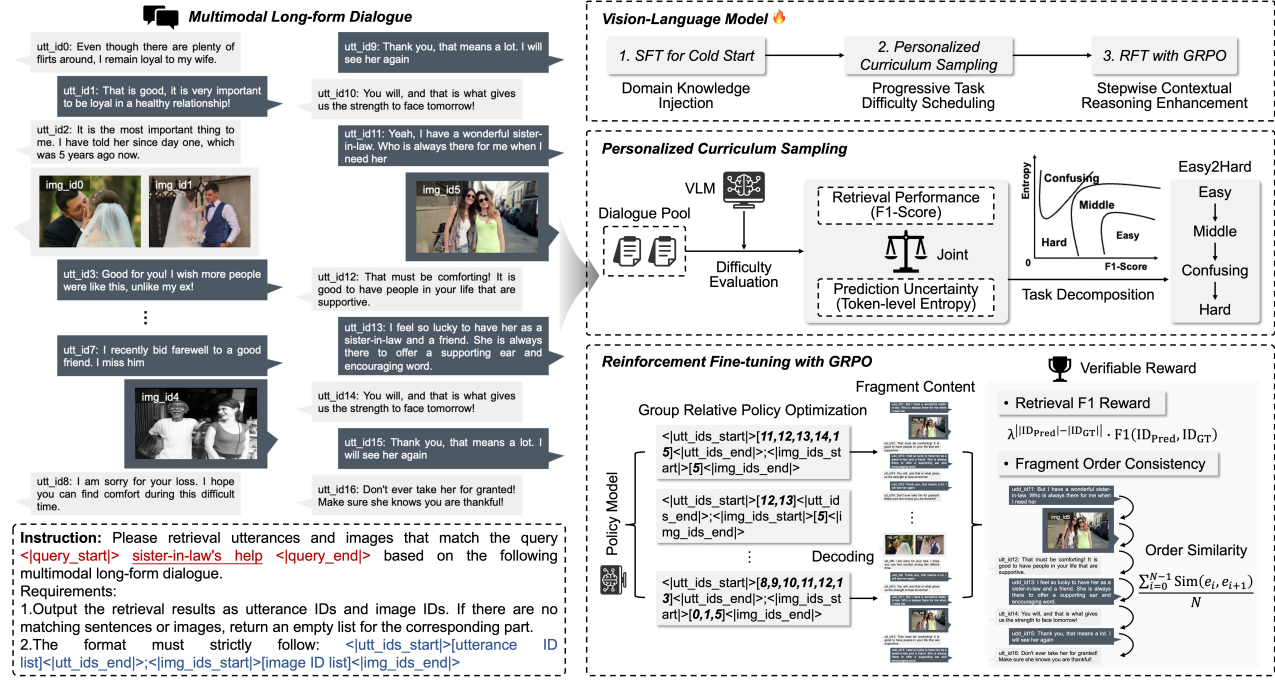


Figure 4: Overview of the F<sup>2</sup>RVL framework for multimodal long-form dialogue fragment retrieval. It consists of supervised fine-tuning for fragment-level knowledge injection, personalized curriculum sampling based on retrieval difficulty, and GRPO-based reinforcement learning to jointly enhance retrieval accuracy and fragment semantic coherence.

is trained in two stages: first, supervised fine-tuning injects task-specific knowledge for fragment retrieval; then, GRPO-based reinforcement fine-tuning is conducted with a multi-objective reward that promotes semantic precision and contextual coherence. To stabilize training and enhance long-range reasoning, samples are organized into a difficulty-aware curriculum based on predicted F1 and uncertainty.

## Optimize Fragment Semantic Coherence by GRPO

We adopt a rule-based variant of Group-Relative Policy Optimization (GRPO) (Shao et al. 2024) to align model behavior with human-preferred retrieval patterns. To this end, we design three verifiable reward functions targeting format compliance, retrieval accuracy, and fragment order consistency, jointly guiding the model to generate structured, precise, and contextually coherent outputs.

**Format Reward ( $R_{\text{Format}}$ )**.  $R_{\text{Format}}$  encourages the model to strictly adhere to the expected output format:

- $<|\text{utt\_ids\_start}|>[\dots]<|\text{utt\_ids\_end}|>$ ;
- $<|\text{img\_ids\_start}|>[\dots]<|\text{img\_ids\_end}|>$

This binary reward returns 1 only when the output fully matches the required format. A uniqueness constraint is also enforced: if any duplicate IDs are present, the reward is set to 0, even if the overall format appears correct.

**Retrieval F1 Reward ( $R_{\text{F1}}$ )**. To encourage precise yet well-scoped retrieval, we design a reward function based on the F1 score with an exponential penalty on length deviation. It considers both utterance and image ID overlaps between predictions and ground truth, while explicitly penalizing

over- and under-retrieval:

$$R_{\text{F1}} = \sum_{m \in \{\text{utt, img}\}} \lambda_m \cdot \text{F1}(I_m^{\text{pred}}, I_m^{\text{gt}}) \cdot \gamma^{|I_m^{\text{pred}}| - |I_m^{\text{gt}}|} \quad (2)$$

where  $I_m^{\text{pred}}$  and  $I_m^{\text{gt}}$  denote the predicted and ground-truth ID sets, respectively. The weighting factors  $\lambda$  balances modality importance. The penalty base  $\gamma \in (0, 1)$  modulates the severity of the length penalty, which increases exponentially with deviation in prediction length.

**Fragment Order Consistency ( $R_{\text{Fragment}}$ )**. To encourage semantically coherent, contextually aligned fragment retrieval, we propose a reward based on cross-modal fragment order consistency. It evaluates whether the retrieved utterances and images maintain the natural progression of information, which is especially important in long conversations with intertwined modalities. Given the predicted sets of utterance and image IDs, we first locate the corresponding textual and visual elements in the original dialogue and encode them into a unified embedding space with CLIP. These embeddings are then interleaved and temporally ordered according to their original positions within the dialogue, forming a cross-modal sequence  $\{e_1, e_2, \dots, e_N\}$ . The reward is defined as the average pairwise cosine similarity between adjacent embeddings in this sequence:

$$R_{\text{Fragment}} = \frac{1}{N-1} \sum_{i=1}^{N-1} \cos(\mathbf{e}_i, \mathbf{e}_{i+1}) \quad (3)$$

If the sequence length  $N$  is less than 2, a fallback reward (i.e., 0.5) is returned.

Model	In-domain Val Set (MLDR)				Real-domain Test Set (WeChat)			
	Precision(%)	Recall(%)	F1(%)	MCC(%)	Precision(%)	Recall(%)	F1(%)	MCC(%)
CLIP-Embedding <sup>†</sup>	48.74	30.80	42.73	21.14	20.44	49.91	31.56	17.62
BLIP2-Embedding <sup>†</sup>	31.88	2.96	23.47	0.00	15.22	52.74	25.05	4.94
E5-V-Embedding <sup>†</sup>	53.85	48.83	51.82	28.92	30.33	47.13	36.99	24.40
GME-Embedding <sup>†</sup>	62.27	23.75	35.52	24.17	29.63	53.11	38.22	26.68
Qwen2.5-VL-7B <sup>†</sup>	21.20	4.27	7.84	0.00	10.22	16.34	12.58	0.00
MiMo-7B-RL <sup>†</sup>	67.68	55.19	61.30	45.52	41.74	24.48	30.94	23.68
Qwen2.5-VL-72B <sup>†</sup>	61.11	67.14	64.09	44.61	32.55	36.95	36.60	25.26
Doubao-Seed-1.6 <sup>†</sup>	73.83	42.19	54.67	42.57	55.22	28.47	38.63	34.06
Claude-Sonnet-4 <sup>†</sup>	67.21	58.09	62.80	46.57	51.15	40.88	46.30	40.50
GPT-4o <sup>†</sup>	70.43	52.49	60.32	45.91	56.11	41.82	48.89	42.85
Gemini-2.5-Flash <sup>†</sup>	70.18	69.30	69.87	54.66	51.89	49.80	53.21	48.22
Ovis2-2B*	76.97	42.48	54.82	43.98	40.83	54.51	46.69	33.16
mPLUG-Owl13-2B	74.86	83.18	78.88	67.59	18.35	45.99	26.37	11.61
Qwen2-VL-2B	74.97	92.99	83.07	74.18	23.20	76.03	36.65	26.55
Qwen2.5-VL-3B	80.35	91.41	85.57	77.98	33.75	75.82	47.60	39.56
LLaVA-1.5-7B-hf*	68.15	92.06	78.43	66.95	20.91	81.27	33.61	22.99
MiMo-7B-RL	80.90	93.46	86.71	79.78	49.46	48.22	49.05	41.84
Qwen2-VL-7B	83.15	90.72	86.81	79.92	42.80	69.60	53.54	45.75
Qwen2.5-VL-7B	81.52	91.42	86.23	79.00	39.99	71.30	51.71	43.65
InternVL3-8B*	80.67	92.98	86.43	79.35	34.08	75.52	47.07	36.65
DeepSeek-VL2-Small-16B	77.52	91.13	83.82	75.23	47.43	19.48	27.91	24.51
<b>F<sup>2</sup>RVLM-Qwen2-VL-2B</b>	79.64	89.55	84.35	76.07	26.97	72.00	40.46	30.90
<b>F<sup>2</sup>RVLM-Qwen2.5-VL-3B</b>	82.74	91.65	87.00	80.19	45.24	70.86	55.60	48.09
<b>F<sup>2</sup>RVLM-Qwen2-VL-7B</b>	<b>84.02</b>	90.67	<b>87.25</b>	<b>80.60</b>	<b>57.21</b>	67.46	<b>62.07</b>	<b>55.46</b>
<b>F<sup>2</sup>RVLM-Qwen2.5-VL-7B</b>	83.24	91.60	87.24	80.55	54.83	65.16	59.60	52.39

Table 2: Comparison with popular VLMs on the MLDR validation set and WeChat test set. “†” indicates zero-shot inference without MLDR fine-tuning. “\*” indicates models limited by context length, evaluated via sliding-window inference.

### Difficulty-aware Curriculum Sampling

Fragment structures in long-form dialogues differ in the distribution of their internal elements: some comprise utterances or images that are tightly clustered within adjacent turns, while others span sparsely across distant positions. This variation significantly affects retrieval difficulty, clustered fragments are generally easier to locate, whereas dispersed ones are harder to handle reliably.

To leverage this inherent difficulty hierarchy, we adopt a difficulty-aware curriculum sampling that dynamically quantifies instance difficulty based on predicted F1 scores and confidence. Training begins with high-confidence, high-F1 samples (i.e., easy cases) and gradually incorporates harder ones with lower scores. This progressive schedule enables the model to first master reasoning in dense contexts, then adapt to long-range, complex scenarios, mirroring the incremental nature of human learning. Specifically, for each training sample  $x_i$ , we compute two indicators utilizing a cold-start model: (1) **Retrieval F1 Score**  $f_i$ : measures overlap between predicted and ground-truth utterance/image ID sets; and (2) **Prediction Entropy**  $h_i$ : quantifies uncertainty as the average entropy of predicted token distributions. Each instance is then assigned a difficulty level based on the following criteria:

$$d_i = \begin{cases} \text{Easy,} & f_i \geq Q_{0.75}^{(f)} \text{ and } h_i \leq Q_{0.25}^{(h)} \\ \text{Confusing,} & f_i \leq Q_{0.25}^{(f)} \text{ and } h_i \geq Q_{0.75}^{(h)} \\ \text{Hard,} & f_i \leq Q_{0.25}^{(f)} \text{ and } h_i \leq Q_{0.25}^{(h)} \\ \text{Medium,} & \text{otherwise} \end{cases} \quad (4)$$

Here,  $Q_p^{(f)}$  and  $Q_p^{(h)}$  denote the  $p$ -th percentiles of F1 and entropy distributions. “Easy” samples are confident and cor-

rect, “Confusing” are uncertain and incorrect, while “Hard” are incorrect yet overconfident.

## Experiments

### Experimental Settings

**Models & Details.** We implement F<sup>2</sup>RVLM based on the ms-swift (Zhao et al. 2024) framework, using Qwen-VL-series as the backbone with 2B, 3B, and 7B parameters. Parameter-efficient fine-tuning is conducted on the MLDR dataset via LoRA (Hu et al. 2022). For evaluation, we compare F<sup>2</sup>RVLM against a comprehensive set of VLMs, including proprietary models such as GPT-4o (Jaech et al. 2024), Gemini-2.5 (Comanici et al. 2025), Doubao-Seed-1.6 (Guo et al. 2025a), and Claude-Sonnet-4; open-source generation-based models including LLaVa (Liu et al. 2023b), Qwen-VL-series (Wang et al. 2024), DeepSeek-VL2-series (Wu et al. 2024), InternVL3-series (Chen et al. 2024), Ovis2 (Lu et al. 2024), Owl13 (Ye et al. 2024), and Mimo-VL (Xiaomi 2025); as well as embedding-based models such as CLIP (Radford et al. 2021), BLIP-2 (Li et al. 2023), E5-V (Jiang et al. 2024a), and GME (Zhang et al. 2024). Open-source models are fine-tuned on MLDR using SFT, while proprietary and embedding-based models are evaluated in inference-only mode. Full implementation details are provided in the Appendix B.

**Metrics.** We evaluate fragment-level retrieval performance utilizing four metrics: Precision, Recall, F1 Score, and Matthews Correlation Coefficient (MCC), computed separately for utterance IDs and image IDs. To obtain unified scores, we average the F1 and MCC values across both modalities and calculate the harmonic mean of Precision and Recall to reflect joint retrieval performance.

Model	#Params	Fragment Consis.	Query Sim.
Doubao-Seed-1.6 <sup>†</sup>		27.89	31.06
Gemini-2.5-Flash <sup>†</sup>	Closed	37.67	41.44
Claude-Sonnet-4 <sup>†</sup>	-Source	42.29	46.64
GPT-4o <sup>†</sup>		43.17	48.21
Qwen2.5-VL <sup>†</sup>	72B	45.98	48.49
DeepSeek-VL2-Small	16B	12.52	13.67
MiMo-VL-RL	7B	34.69	36.69
Qwen2-VL	7B	55.28	59.49
Qwen2.5-VL	7B	54.81	58.39
<b>F<sup>2</sup>RVLM</b>	3B	<b>60.53</b>	<b>61.18</b>

Table 3: Comparison with popular VLMs on the real-domain WeChat test set, evaluated by Fragment Order Consistency and Query-Fragment Similarity. “<sup>†</sup>” indicates zero-shot inference without MLDR fine-tuning.

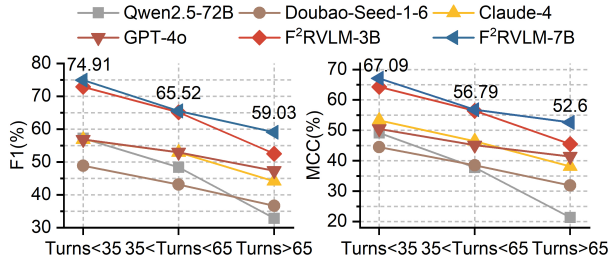


Figure 5: Performance comparison across dialogue turn groups on the real-domain WeChat test set.

### Comparison with Popular VLMs

**Overall Retrieval Performance.** Table 2 summarizes fragment-level retrieval results on the in-domain MLDR validation set and the real-domain WeChat test set. Key observations include: (1) F<sup>2</sup>RVLM achieves SOTA performance in both domains. The 7B variant tops MLDR with 87.25% F1, and leads on WeChat with 62.07% F1. Its 3B version also outperforms larger competitors such as MiMo-7B-RL, and GPT-4o. (2) MLDR Fine-tuning significantly boosts cross-domain retrieval. Qwen2.5-VL-7B improves from 12.58% (zero-shot) to 51.71% F1 on WeChat after MLDR tuning, demonstrating MLDR’s value as a supervised resource for fragment retrieval. Moreover, F<sup>2</sup>RVLM offers less performance degradation from MLDR to WeChat compared to other models, indicating stronger generalization in real-world long-form dialogues. (3) Detailed metric results, qualitative analysis, and further discussion on generalization can be found in Appendix.C.

**Discussion about Recall Metric.** While models like LLaVA achieve higher recall, they often sacrifice precision by retrieving many irrelevant fragments. In contrast, our model incorporates a penalty term in the  $R_{F1}$  to suppress over-retrieval, encouraging the selection of fewer but more semantically consistent fragments, better aligned with human preferences and fragment-level retrieval objectives.

**Fragment-level Consistency and Alignment.** To assess VLMs’ ability to capture dialogue structure and semantic alignment, we introduce two metrics on the WeChat test set: Fragment Order Consistency (average cosine similarity between adjacent retrieved elements) and Query-Fragment Similarity (average similarity between the query and each retrieved element), as reported in Table 3. F<sup>2</sup>RVLM achieves the highest scores on both, outperforming larger open- and

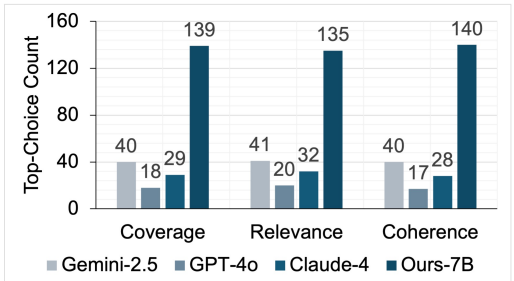


Figure 6: Human subjective evaluation results on the WeChat test set. We randomly sample 200 dialogues and ask expert annotators to select the top-performing model across three criteria: Coverage, Relevance, and Coherence.

$R_{F1}$	$R_{Fragment}$	Curriculum	In-domain		Real-domain	
			F1(%)	MCC(%)	F1(%)	MCC(%)
✗	✗	✓	86.02	78.69	53.39	46.07
✓	✗	✓	86.39	79.24	54.68	47.41
✓	✓	✗	84.69	77.53	50.65	43.71
✓	✓	✓	<b>87.00</b>	<b>80.19</b>	<b>55.60</b>	<b>48.09</b>

Table 4: Ablation study on reward components and curriculum sampling on MLDR validation and WeChat test sets.

closed-source models. This demonstrates its superior ability to retrieve coherent, semantically aligned fragments, enabled by the order-consistency reward in GRPO training.

**Discussion about Dialogue Turns.** Fig.5 reports model performance on the WeChat test set across short (<35 turns), medium (35–65 turns), and long (>65 turns) dialogues. F<sup>2</sup>RVLM-7B (Qwen2) consistently achieves the highest F1 and MCC scores as dialogue turn increases, with minimal performance degradation compared to other models, which demonstrates its robustness in long-context reasoning.

**Subjective Results.** We conduct a human evaluation on 200 dialogues from the WeChat test set, comparing our 7B model against Gemini-2.5, GPT-4o, and Claude-4 across three criteria: coverage, relevance, and fragment coherence (detailed definitions are provided in Appendix.C). As depicted in Fig.6, our model is consistently preferred by annotators, receiving the highest top-choice counts in all aspects, demonstrating superior semantic completeness, alignment, and fluency in real-world dialogue retrieval.

### Ablation Results

This section presents ablation studies to evaluate the effectiveness of the proposed reward functions and personalized curriculum learning, focusing on joint F1 and MCC metrics (Table 4). (1) Replacing standard accuracy with  $R_{F1}$  significantly improves performance, while incorporating fragment order consistency  $R_{Fragment}$  further enhances cross-domain F1 and MCC, highlighting the role of intra-fragment semantic consistency. (2) Integrating difficulty-aware curriculum sampling into GRPO yields consistent gains: in-domain F1 improves from 84.69% to 87.00%, and real-domain F1 from 50.65% to 55.60%, validating the effectiveness of progressive learning from easier to harder samples. (3) We also explore different training ratios of SFT and GRPO-based RFT, with detailed results provided in Appendix.C.

## Conclusion

This study defines Fine-grained Fragment Retrieval (FFR) to locate semantically coherent utterance-image fragments from long-form multimodal dialogues. To support this task, we construct MLDR, the longest-turn multimodal dialogue dataset to date, along with a real-world WeChat test set. Based on these resources, we propose F<sup>2</sup>RVLM, a generation-based retrieval model trained with GRPO-based reinforcement learning to encourage semantically coherent fragment prediction. F<sup>2</sup>RVLM surpasses popular VLMs, achieving superior accuracy in both in-domain and real-world evaluations.

## References

Achiam, J.; Adler, S.; Agarwal, S.; Ahmad, L.; Akkaya, I.; Aleman, F. L.; Almeida, D.; Altenschmidt, J.; Altman, S.; Anadkat, S.; et al. 2023. Gpt-4 technical report. *arXiv preprint arXiv:2303.08774*.

Chen, Y.; Fan, W.; Xing, X.; Pang, J.; Huang, M.; Han, W.; Tie, Q.; and Xu, X. 2022. CPED: A Large-Scale Chinese Personalized and Emotional Dialogue Dataset for Conversational AI. *arXiv preprint arXiv:2205.14727*.

Chen, Z.; Wu, J.; Wang, W.; Su, W.; Chen, G.; Xing, S.; Zhong, M.; Zhang, Q.; Zhu, X.; Lu, L.; et al. 2024. Internvl: Scaling up vision foundation models and aligning for generic visual-linguistic tasks. In *Proceedings of the IEEE/CVF Conference on Computer Vision and Pattern Recognition*, 24185–24198.

Choe, S.; Oh, J.; and Yang, J. 2025. Multimodal Contrastive Learning for Dialogue Embeddings with Global and Local Views. In *Pacific-Asia Conference on Knowledge Discovery and Data Mining*, 155–166. Springer.

Comanici, G.; Bieber, E.; Schaeckermann, M.; Pasupat, I.; Sachdeva, N.; Dhillon, I.; Blstein, M.; Ram, O.; Zhang, D.; Rosen, E.; et al. 2025. Gemini 2.5: Pushing the frontier with advanced reasoning, multimodality, long context, and next generation agentic capabilities. *arXiv preprint arXiv:2507.06261*.

Feng, J.; Sun, Q.; Xu, C.; Zhao, P.; Yang, Y.; Tao, C.; Zhao, D.; and Lin, Q. 2023. MMDialog: A Large-scale Multi-turn Dialogue Dataset Towards Multi-modal Open-domain Conversation. In *Proceedings of the 61st Annual Meeting of the Association for Computational Linguistics (Volume 1: Long Papers)*, 7348–7363.

Feng, K.; Gong, K.; Li, B.; Guo, Z.; Wang, Y.; Peng, T.; Wu, J.; Zhang, X.; Wang, B.; and Yue, X. 2025. Video-r1: Reinforcing video reasoning in llms. *arXiv preprint arXiv:2503.21776*.

Guo, D.; Wu, F.; Zhu, F.; Leng, F.; Shi, G.; Chen, H.; Fan, H.; Wang, J.; Jiang, J.; Wang, J.; et al. 2025a. Seed1. 5-vl technical report. *arXiv preprint arXiv:2505.07062*.

Guo, D.; Yang, D.; Zhang, H.; Song, J.; Zhang, R.; Xu, R.; Zhu, Q.; Ma, S.; Wang, P.; Bi, X.; et al. 2025b. Deepseek-r1: Incentivizing reasoning capability in llms via reinforcement learning. *arXiv preprint arXiv:2501.12948*.

Hu, E. J.; Shen, Y.; Wallis, P.; Allen-Zhu, Z.; Li, Y.; Wang, S.; Wang, L.; Chen, W.; et al. 2022. Lora: Low-rank adaptation of large language models. *ICLR*, 1(2): 3.

Huang, W.; Jia, B.; Zhai, Z.; Cao, S.; Ye, Z.; Zhao, F.; Xu, Z.; Hu, Y.; and Lin, S. 2025. Vision-r1: Incentivizing reasoning capability in multimodal large language models. *arXiv preprint arXiv:2503.06749*.

Jaech, A.; Kalai, A.; Lerer, A.; Richardson, A.; El-Kishky, A.; Low, A.; Helyar, A.; Madry, A.; Beutel, A.; Carney, A.; et al. 2024. Openai o1 system card. *arXiv preprint arXiv:2412.16720*.

Jiang, T.; Song, M.; Zhang, Z.; Huang, H.; Deng, W.; Sun, F.; Zhang, Q.; Wang, D.; and Zhuang, F. 2024a. E5-v: Universal embeddings with multimodal large language models. *arXiv preprint arXiv:2407.12580*.

Jiang, Z.; Meng, R.; Yang, X.; Yavuz, S.; Zhou, Y.; and Chen, W. 2024b. VLM2Vec: Training Vision-Language Models for Massive Multimodal Embedding Tasks. *arXiv preprint arXiv:2410.05160*.

Lee, N.; Shin, S.; Choo, J.; Choi, H.-J.; and Myaeng, S.-H. 2021. Constructing Multi-Modal Dialogue Dataset by Replacing Text with Semantically Relevant Images. In *Proceedings of the 59th Annual Meeting of the Association for Computational Linguistics and the 11th International Joint Conference on Natural Language Processing (Volume 2: Short Papers)*, 897–906.

Lee, Y.-J.; Ko, B.; Kim, H.-G.; Hyeon, J.; and Choi, H.-J. 2024. DialogCC: An Automated Pipeline for Creating High-Quality Multi-Modal Dialogue Dataset. In *Proceedings of the 2024 Conference of the North American Chapter of the Association for Computational Linguistics: Human Language Technologies (Volume 1: Long Papers)*, 1938–1963.

Lee, Y.-J.; Lee, D.; Sung, J. W.; Hyeon, J.; and Choi, H.-J. 2023. Large Language Models can Share Images, Too! *arXiv preprint arXiv:2310.14804*.

Li, J.; Li, D.; Savarese, S.; and Hoi, S. 2023. Blip-2: Bootstrapping language-image pre-training with frozen image encoders and large language models. In *International conference on machine learning*, 19730–19742. PMLR.

Li, J.; Li, D.; Xiong, C.; and Hoi, S. 2022. Blip: Bootstrapping language-image pre-training for unified vision-language understanding and generation. In *International conference on machine learning*, 12888–12900. PMLR.

Lin, H.; Ruan, L.; Xia, W.; Liu, P.; Wen, J.; Xu, Y.; Hu, D.; Song, R.; Zhao, W. X.; Jin, Q.; et al. 2023. TikTalk: a video-based dialogue dataset for multi-modal chitchat in real world. In *Proceedings of the 31st ACM International Conference on Multimedia*, 1303–1313.

Liu, H.; Li, C.; Wu, Q.; and Lee, Y. J. 2023a. Visual instruction tuning. *Advances in neural information processing systems*, 36: 34892–34916.

Liu, H.; Li, C.; Wu, Q.; and Lee, Y. J. 2023b. Visual Instruction Tuning. In *NeurIPS*.

Liu, Y.; Zhang, Y.; Cai, J.; Jiang, X.; Hu, Y.; Yao, J.; Wang, Y.; and Xie, W. 2025a. Lamra: Large multimodal model

as your advanced retrieval assistant. In *Proceedings of the Computer Vision and Pattern Recognition Conference*, 4015–4025.

Liu, Z.; Sun, Z.; Zang, Y.; Dong, X.; Cao, Y.; Duan, H.; Lin, D.; and Wang, J. 2025b. Visual-rft: Visual reinforcement fine-tuning. *arXiv preprint arXiv:2503.01785*.

Liu, Z.; Xiong, C.; Lv, Y.; Liu, Z.; and Yu, G. 2022. Universal vision-language dense retrieval: Learning a unified representation space for multi-modal retrieval. *arXiv preprint arXiv:2209.00179*.

Lu, S.; Li, Y.; Chen, Q.-G.; Xu, Z.; Luo, W.; Zhang, K.; and Ye, H.-J. 2024. Ovis: Structural Embedding Alignment for Multimodal Large Language Model. *arXiv:2405.20797*.

Meng, Y.; Wang, S.; Han, Q.; Sun, X.; Wu, F.; Yan, R.; and Li, J. 2020. Openvial: A large-scale, open-domain dialogue dataset with visual contexts. *arXiv preprint arXiv:2012.15015*.

Peng, Y.; Zhang, G.; Zhang, M.; You, Z.; Liu, J.; Zhu, Q.; Yang, K.; Xu, X.; Geng, X.; and Yang, X. 2025. Lmm-r1: Empowering 3b lmms with strong reasoning abilities through two-stage rule-based rl. *arXiv preprint arXiv:2503.07536*.

Radford, A.; Kim, J. W.; Hallacy, C.; Ramesh, A.; Goh, G.; Agarwal, S.; Sastry, G.; Askell, A.; Mishkin, P.; Clark, J.; et al. 2021. Learning transferable visual models from natural language supervision. In *International conference on machine learning*, 8748–8763. PMLR.

Shao, Z.; Wang, P.; Zhu, Q.; Xu, R.; Song, J.; Bi, X.; Zhang, H.; Zhang, M.; Li, Y.; Wu, Y.; et al. 2024. Deepseekmath: Pushing the limits of mathematical reasoning in open language models. *arXiv preprint arXiv:2402.03300*.

Shen, H.; Liu, P.; Li, J.; Fang, C.; Ma, Y.; Liao, J.; Shen, Q.; Zhang, Z.; Zhao, K.; Zhang, Q.; et al. 2025. Vlm-r1: A stable and generalizable r1-style large vision-language model. *arXiv preprint arXiv:2504.07615*.

Shuster, K.; Humeau, S.; Bordes, A.; and Weston, J. 2020. Image-Chat: Engaging Grounded Conversations. In *Proceedings of the 58th Annual Meeting of the Association for Computational Linguistics*, 2414–2429.

Tan, H.; Ji, Y.; Hao, X.; Lin, M.; Wang, P.; Wang, Z.; and Zhang, S. 2025. Reason-rft: Reinforcement fine-tuning for visual reasoning. *arXiv preprint arXiv:2503.20752*.

Wang, B.; Du, Y.; Liang, B.; Bai, Z.; Yang, M.; Wang, B.; Wong, K.-F.; and Xu, R. 2025a. A new formula for sticker retrieval: Reply with stickers in multi-modal and multi-session conversation. In *Proceedings of the AAAI Conference on Artificial Intelligence*, volume 39, 25327–25335.

Wang, H.; Qu, C.; Huang, Z.; Chu, W.; Lin, F.; and Chen, W. 2025b. Vl-rethinker: Incentivizing self-reflection of vision-language models with reinforcement learning. *arXiv preprint arXiv:2504.08837*.

Wang, P.; Bai, S.; Tan, S.; Wang, S.; Fan, Z.; Bai, J.; Chen, K.; Liu, X.; Wang, J.; Ge, W.; et al. 2024. Qwen2-vl: Enhancing vision-language model’s perception of the world at any resolution. *arXiv preprint arXiv:2409.12191*.

Wei, C.; Chen, Y.; Chen, H.; Hu, H.; Zhang, G.; Fu, J.; Ritter, A.; and Chen, W. 2024a. Uniir: Training and benchmarking universal multimodal information retrievers. In *European Conference on Computer Vision*, 387–404. Springer.

Wei, Z.; Liao, L.; Du, X.; and Xiang, X. 2024b. Balancing Visual Context Understanding in Dialogue for Image Retrieval. In *EMNLP 2024-2024 Conference on Empirical Methods in Natural Language Processing, Findings of EMNLP 2024*, 7929–7942. Association for Computational Linguistics (ACL).

Wu, Z.; Chen, X.; Pan, Z.; Liu, X.; Liu, W.; Dai, D.; Gao, H.; Ma, Y.; Wu, C.; Wang, B.; et al. 2024. Deepseek-vl2: Mixture-of-experts vision-language models for advanced multimodal understanding. *arXiv preprint arXiv:2412.10302*.

Xiaomi, L.-C.-T. 2025. MiMo-VL Technical Report. *arXiv:2506.03569*.

Yang, A.; Li, A.; Yang, B.; Zhang, B.; Hui, B.; Zheng, B.; Yu, B.; Gao, C.; Huang, C.; Lv, C.; et al. 2025. Qwen3 technical report. *arXiv preprint arXiv:2505.09388*.

Ye, J.; Xu, H.; Liu, H.; Hu, A.; Yan, M.; Qian, Q.; Zhang, J.; Huang, F.; and Zhou, J. 2024. mPLUG-Owl3: Towards Long Image-Sequence Understanding in Multi-Modal Large Language Models. *arXiv:2408.04840*.

Yin, Z.; Hui, B.; Yang, M.; Huang, F.; and Li, Y. 2024. Dialclip: Empowering clip as multi-modal dialog retriever. In *ICASSP 2024-2024 IEEE International Conference on Acoustics, Speech and Signal Processing (ICASSP)*, 12421–12425. IEEE.

Yu, Q.; Zhang, Z.; Zhu, R.; Yuan, Y.; Zuo, X.; Yue, Y.; Dai, W.; Fan, T.; Liu, G.; Liu, L.; et al. 2025. Dapo: An open-source llm reinforcement learning system at scale. *arXiv preprint arXiv:2503.14476*.

Yue, Y.; Yuan, Y.; Yu, Q.; Zuo, X.; Zhu, R.; Xu, W.; Chen, J.; Wang, C.; Fan, T.; Du, Z.; et al. 2025. Vapo: Efficient and reliable reinforcement learning for advanced reasoning tasks. *arXiv preprint arXiv:2504.05118*.

Zang, X.; Liu, L.; Wang, M.; Song, Y.; Zhang, H.; and Chen, J. 2021. PhotoChat: A Human-Human Dialogue Dataset With Photo Sharing Behavior For Joint Image-Text Modeling. In *Proceedings of the 59th Annual Meeting of the Association for Computational Linguistics and the 11th International Joint Conference on Natural Language Processing (Volume 1: Long Papers)*, 6142–6152.

Zhang, X.; Zhang, Y.; Xie, W.; Li, M.; Dai, Z.; Long, D.; Xie, P.; Zhang, M.; Li, W.; and Zhang, M. 2024. GME: Improving Universal Multimodal Retrieval by Multimodal LLMs. *arXiv preprint arXiv:2412.16855*.

Zhang, Y.; Yu, Y.; Guo, Q.; Wang, B.; Zhao, D.; Uprety, S.; Song, D.; Li, Q.; and Qin, J. 2023. CMMA: benchmarking multi-affection detection in chinese multi-modal conversations. *Advances in Neural Information Processing Systems*, 36: 18794–18805.

Zhao, J.; Zhang, T.; Hu, J.; Liu, Y.; Jin, Q.; Wang, X.; and Li, H. 2022. M3ED: Multi-modal Multi-scene Multi-label Emotional Dialogue Database. In *Proceedings of the 60th*

*Annual Meeting of the Association for Computational Linguistics (Volume 1: Long Papers)*, 5699–5710.

Zhao, Y.; Huang, J.; Hu, J.; Wang, X.; Mao, Y.; Zhang, D.; Jiang, Z.; Wu, Z.; Ai, B.; Wang, A.; Zhou, W.; and Chen, Y. 2024. SWIFT: A Scalable lightWeight Infrastructure for Fine-Tuning. arXiv:2408.05517.

Zheng, Y.; Chen, G.; Liu, X.; and Sun, J. 2022. MMChat: Multi-Modal Chat Dataset on Social Media. In *Proceedings of the Thirteenth Language Resources and Evaluation Conference*, 5778–5786.

## Appendix Overview

The Supplementary Materials offer additional insights and experimental details that support the main paper. The content is organized as follows:

- **Appendix A: Dataset Construction and Analysis**
  - **A1. MLDR Construction:** Describes the full pipeline for building the MLDR dataset.
  - **A2. WeChat-Based Dataset Construction:** Details the data source, annotation protocol, and licensing for the WeChat test set.
  - **A3. Dataset Statistics and Analysis:** Presents dialogue turn distribution, topic bias analysis, and representative qualitative examples.
- **Appendix B: Implementation Details**
  - **B1. Training and Hyperparameter Settings:** Summarizes training configurations and optimization details.
  - **B2. Model Comparison Settings:** Specifies the fine-tuning and inference setups for all models, including both open-source and proprietary VLMs.
  - **B3. Sliding Window Inference for Long Contexts:** Explains inference strategies for models that cannot process long dialogues directly.
- **Appendix C: Experimental Results and Analysis**
  - **C1. Detailed Comparison of Quantitative Results:** Provides full metric breakdowns on MLDR and WeChat datasets.
  - **C2. Comparison of Qualitative Results:** Compares typical retrieval examples across models.
  - **C3. Cross-Lingual Generalization:** Evaluates performance on an English-translated version of the WeChat test set.
  - **C4. Human Subjective Evaluation Criteria:** Defines coverage, relevance, and coherence metrics used in human evaluation.
  - **C5. Ablation Studies on SFT and GRPO Ratio:** Analyzes the impact of different supervised and reinforcement fine-tuning ratios.

## Appendix A: Dataset Construction and Analysis

### A1. MLDR Construction

This section provides detailed elaboration on the key steps involved in the construction of the MLDR dataset.

**Data Cleaning.** To ensure high-quality long-form construction, we conduct a rigorous cleaning process based on four key filtering standards: (1) Image-Text Consistency: We encode visual and textual content utilizing CLIP and discard samples with low cross-modal similarity. (2) Topic Coherence: Sentence embeddings are obtained utilizing BERT, and K-means clustering is applied to filter out dialogues that deviate from a central topic. (3) Dialogue Turn Structure: Each dialogue must contain at least three turns in

a “User1–User2–User1” pattern to ensure basic conversational flow. (4) Image Quality: We filter out images with resolutions below 500 pixels or with extreme aspect ratios (greater than 7.5), ensuring visual quality.

**Dialogue Triplet Semantic Matching.** To generate coherent long-form dialogues from multiple short dialogues, we propose a three-step triplet-based semantic matching strategy. This process ensures both topic continuity and multimodal alignment, and includes the following steps:

- Trial Screening of Text Semantic: For each cleaned short dialogue  $D_A$ , we first perform textual semantic screening. We encode all textual content (including image captions) using a pretrained BERT model and compute the mean sentence embedding for each dialogue. Cosine similarity is then calculated between  $D_A$ ’s embedding and the embeddings of all other candidate dialogues. Based on this initial similarity score, we select the Top- $K$  (where  $K = 50$ ) most semantically relevant dialogues.
- Refined Screening of Multimodal Semantic: Next, we perform multimodal semantic refinement for the Top- $K$  dialogues selected in the first step. Using CLIP, we separately encode both textual and visual content, calculating the cosine similarity for each modality. These similarities are then combined with weighted scores (i.e., 0.7 for text and 0.3 for image) to obtain the final multimodal similarity score. From this, we select the Top-2 dialogues  $\{D_B^1, D_B^2\}$ , based on this refined multimodal score.
- Triplet Construction: For each selected dialogue  $D_B^i$  ( $i = 1, 2$ ), we repeat the above two-stage matching process to retrieve the Top-2 most semantically and multimodally relevant dialogues, denoted as  $\{D_C^{i,1}, D_C^{i,2}\}$ . This results in 4 distinct triplets:

$$D_A \rightarrow D_B^i \rightarrow D_C^{i,j}, \quad i = 1, 2; \quad j = 1, 2 \quad (5)$$

These triplets provide a structural foundation for generating extended dialogues, ensuring both semantic and multimodal coherence. Notably, each dialogue  $D_A$ ,  $D_B$ , and  $D_C$  in a triplet must be mutually disjoint in terms of both dialogue ID and image content, ensuring that each triplet represents unique and non-duplicate information.

**Long-form Dialogue Generation.** To convert semantically aligned triplets into coherent long-form dialogues, we employ the Qwen3 256B (Yang et al. 2025) large language model under a structured prompt template (Fig.7). The generation process adheres to the following principles: (1) Preserve the original multimodal content and semantics while enhancing fluency and readability. (2) Insert natural transition utterances to ensure coherent topic progression and stylistic consistency across dialogue segments. (3) Translating all content into fluent and contextually appropriate Chinese, aligned with real-world conversational norms. This process enables the synthesis of high-quality, semantically coherent, and structurally complete Chinese multimodal long-form dialogues, which form the foundation for subsequent retrieval and understanding tasks.

**Multi-Granularity Annotation.** To enable fine-grained semantic retrieval over long-form multimodal dialogues, we

Datasets	Modalites	Dialogue Type	Dialogue Source	Language	Dialogues	Images	Turns	Turn/Dialog	Topic/Dialog
ImageChat (Shuster et al. 2020)	v, t	image-grounded	crowdsourcing	English	201,779	201,779	400,853	1.98	1.00
OpenViDial (Meng et al. 2020)	v, t	image-grounded	moviesTVs	English	1,100,000	1,100,000	1,100,000	1.00	1.00
PhotoChat (Zang et al. 2021)	v, t	image-sharing	crowdsourcing	English	11,820	10,479	150,138	12.74	1.00
MMDial (Lee et al. 2021)	v, t	image-sharing	text datasets	English	17,679	13,288	187,421	11.56	1.00
MMDialog (Feng et al. 2023)	v, t	image-sharing	social media	English	1,079,117	1,556,868	4,920,000	4.56	1.00
DialogCC (Lee et al. 2024)	v, t	image-sharing	text datasets	English	83,209	129,802	676,181	8.20	1.00
MMChat (Zheng et al. 2022)	v, t	image-grounded	social media	Chinese	120,840	204,320	314,130	2.59	1.00
M3ED (Zhao et al. 2022)	a, v, t	video-grounded	TVs	Chinese	990	-	9082	9.17	1.00
CPED (Chen et al. 2022)	a, v, t	video-grounded	TVs	Chinese	12,000	-	133,000	11.08	1.00
CMMA (Zhang et al. 2023)	a, v, t	video-grounded	TVs	Chinese	3,000	-	21,795	7.27	1.00
TikTalk (Lin et al. 2023)	a, v, t	video-grounded	social media	Chinese	367,670	38,703 videos	826,752	2.25	1.00
<b>Our Dataset</b>	v, t	image-sharing	text datasets	Chinese	37,030	194,543	942,414	<b>25.45</b>	<b>3.00</b>

Table 5: Summary of main multimodal dialogue datasets. Datasets are categorized by modality (audio (a), visual (v), and textual (t)), dialogue type (image/video-grounded vs. image-sharing), source, and language. Our MLDR dataset features significantly longer dialogues and richer topic transitions, better reflecting real-world human communication scenarios.

#### Prompt Template for Long-form Dialogue Generation:

You are a professional assistant for integrating dual-speaker dialogues. Your task is to merge the following three short dialogues into one coherent long-form conversation. Please strictly follow the rules below:

1. Unify Speakers: All speakers across the three dialogues must be unified as "User1" and "User2", while preserving each individual's original speaking style.
2. Preserve Content: Retain the full content of all three dialogues without omission. If any information is missing or unclear, make reasonable and contextually appropriate completions.
3. Accurate Translation: Translate each utterance into fluent and natural Chinese, ensuring semantic accuracy and alignment with everyday conversational tone.
4. Special Tag Handling: Any sentence containing the tag '<IMAGE SHARING>caption<IMAGE SHARING>' should remain as a standalone sentence. Do not translate it, do not merge it with other utterances, and do not modify its text or replace names with "User1" or "User2".
5. Logical Ordering: Rearrange the three dialogues if necessary to ensure a clear and logical flow in the merged conversation.
6. Transition Sentences: One of the speakers should insert two natural and contextually appropriate transition sentences to smoothly connect the different topics of the original dialogues.
7. Expression Optimization: Without altering the original meaning or changing the number of utterances, optimize the wording to make the conversation more natural and aligned with real-world dialogue.
8. Output Format: The output must be strictly in JSON format, with all fields complete and correctly typed. Field names and formatting symbols must not contain typos, extra or missing characters. Use the following example as a reference:

```
{
  "dialogue": [ {
    "utterance_idx": 0, // Integer index starting from 0
    "utterance": "Dialogue content", // String type; if the sentence contains <IMAGE SHARING> tags, it should be output exactly as-is
    "speaker": "User1", // Must be either "User1" or "User2" }, // Other dialogue turns should follow this format in order
  }
]
Dialogue 1: {dialogue1_text}
Dialogue 2: {dialogue2_text}
Dialogue 3: {dialogue3_text}
```

Figure 7: Prompt Template for Long-form Dialogue Generation.

design a two-level shared tagging scheme and implement it automatically using a Qwen3 model under structured prompts (see Fig.8). Each sentence and image caption is annotated with (1) a coarse-grained shared tag indicating the high-level domain or scenario (e.g., "banking services", "travel planning"), and (2) a fine-grained shared tag specifying the detailed activity within the domain (e.g., "open savings account"). Both types of tags are required to be shared by at least two utterances or image captions to ensure topic consistency. To support high-quality tagging, Qwen3 is guided by explicit rules including tag reuse, topic-aligned grouping, and context-aware alignment across dialogue turns. This automated annotation process enables efficient semantic disentanglement and facilitates precise retrieval in complex multimodal conversations.

## A2. WeChat-Based Dataset Construction

**Data Source and Licensing Statement.** The real-domain WeChat test set is constructed from naturally occurring image-text conversations voluntarily contributed by 12 participants. These dialogues are not extracted from any internal WeChat databases, but are shared with explicit informed consent from the contributors for academic research purposes. Prior to inclusion, all conversations were thoroughly anonymized and sanitized, with personal identifiers, sensitive content, and inappropriate language removed to ensure privacy protection and ethical compliance. To support responsible use, the dataset will be released under a research-only license. It is strictly prohibited to use the data for commercial applications, product development, or any non-academic purposes. Access to the dataset requires agreement to the accompanying license terms.

**Prompt Template for Multi-Granularity Annotation:**

1. Task Description:

You will be given a long-form dialogue that spans multiple topics and includes image captions. Your task is to annotate each sentence (including image captions) with two types of tags to support efficient segmentation and accurate retrieval of sub-dialogues based on user queries.

2. Tag Types and Annotation Guidelines:

(a) Coarse-Grained Shared

- Definition: Describes the general domain or scene of the dialogue. Each tag must be shared by at least two sentences (including image captions). Each long dialogue must contain at least two different coarse-grained tags.

- Examples:

- Dialogue related to banking: "Banking and Financial Services"

- Dialogue about business negotiations: "Corporate Business Activities"

(b) Fine-Grained Shared Tag

- Definition: Specifies the detailed business activity within the scope of a coarse-grained tag. This tag must also be shared by at least two sentences (including image captions). Each coarse tag must have at least one corresponding fine-grained tag.

- Examples:

- Under "Banking and Financial Services", label sentences about opening a savings account as "Savings Account Opening", and those about interest inquiries as "Savings Interest Consultation".

- Under "Corporate Business Activities", label sentences about meeting preparation as "Business Meeting Preparation", and those about document handover as "Business Document Exchange".

3. Core Annotation Rules:

(a) Tag Hierarchy: Fine-grained tags must be hierarchically linked to corresponding coarse-grained tags (e.g., "Savings Account Opening" should be under "Banking and Financial Services").

Shared Tag Reuse: If multiple sentences (or image captions) relate to the same topic, you must reuse existing shared tag sets to ensure consistency.

(b) Context-Aware Annotation:

- If an image caption is semantically related to adjacent sentences, its coarse and fine tags must align with those context sentences. For example, if the surrounding content involves opening a savings account, the image caption should be tagged with "Banking and Financial Services" (coarse) and "Savings Account Opening" (fine).

- Avoid vague or generic tags such as "XXX Display" for captions. Instead, analyze their contextual meaning and assign accurate business-related tags.

(c) Complete Annotation Requirement: Every sentence (including image captions) must be annotated with all two tag types. No field may be left empty.

(d) Contextual Consistency:

- Ensure that sentences related to the same topic share the same coarse and fine tags (e.g., all sentences about the savings account opening process should use the same tag pair).

- For topic or scene shifts, define new tags accordingly, while maintaining internal consistency within each new topic.

- Carefully consider the sentence semantics, surrounding context, and overall dialogue structure when deciding whether to reuse existing tags or introduce new ones, to avoid tag inconsistency within the same topic.

4. Output Format:

Please output the result in strict \*\*JSON format\*\* with all fields complete and correctly typed. Do not introduce any spelling, formatting, or structure errors. Use the format below as a reference:

```
 {{
  "dialogue": [
    {
      "utterance_idx": 0,
      "coarse_shared_tag": "Banking and Financial Services",
      "fine_shared_tag": "Savings Account Opening",},
      // Other utterances should follow the same format
    ]
  }
}}
```

Long-form dialogue content: {dialogue\_text}

Figure 8: Prompt Template for Multi-Granularity Annotation.

**Annotation Protocol and Quality Control.** To ensure high-quality supervision for real-world fragment retrieval, we recruited 10 trained annotators to label the WeChat test set. Prior to annotation, all annotators received standardized training covering task definitions, multi-granularity labeling rules, and edge case handling. Each dialogue was independently annotated by all annotators to ensure consistency and comprehensive coverage. Following the initial round, we conducted rigorous quality checks to identify inconsistencies and labeling errors. Annotators were required to revise their annotations based on feedback. This iterative process continued until all annotations passed final validation, resulting in a reliable and well-curated benchmark for evaluating fine-grained multimodal retrieval.

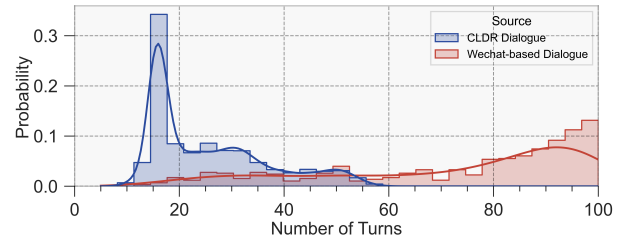


Figure 9: Comparison between the CLDR and WeChat-based datasets in terms of dialogue turn distributions.

### A3. Dataset Statistics and Analysis

**Dataset Cases.** To illustrate the characteristics of different evaluation scenarios, we present representative cases from

both the MLDR and the WeChat test set (as reported in Fig.10-12). The MLDR set contains dialogues with fewer turns and a cleaner structure, while the WeChat test set features long, real-world conversations with many turns and mixed topics, posing greater challenges for retrieval models in maintaining relevance and coherence.

**Topic Distribution Bias in the WeChat Test Set.** As illustrated in Fig.3 in the main body, the WeChat test set exhibits a pronounced skew toward Work & Tech topics, which account for nearly 50% of all annotated dialogues. This bias can be primarily attributed to two factors. (1) The dataset is constructed from real-world conversations voluntarily contributed by 12 participants, most of whom are doctoral students or corporate employees. Their daily communication naturally revolves around professional and technical discussions, resulting in a topic distribution that overrepresents work-related content. (2) In compliance with ethical and privacy considerations, we intentionally filtered out sensitive or highly private conversations (e.g., involving family, personal health, or intimate relationships). This further reduces the proportion of daily-life and emotion-related content.

We acknowledge that this topic bias represents a limitation of the current dataset. While it provides valuable insights into real-world retrieval performance under noisy and task-oriented scenarios, it may not fully capture the diversity of open-domain multimodal interactions. In future iterations, we plan to expand the contributor pool to include participants from more diverse demographics and occupations, and to adopt privacy-preserving mechanisms (e.g., local anonymization) that allow for the safe inclusion of a wider range of topics. This will support the construction of a more balanced and comprehensive real-domain benchmark.

**Dialogue Turn Distribution.** As illustrated in Fig.4, the MLDR and WeChat test sets exhibit markedly different distributions in the number of dialogue turns. The MLDR dialogues are densely concentrated around 15–25 turns, with a sharp peak at around 20, reflecting the synthetic construction of the dataset via triplet concatenation under controlled prompting. This design ensures topic continuity and moderate length, which is beneficial for training and controlled evaluation. In contrast, the WeChat-based dialogues demonstrate a broad and skewed distribution, ranging from short to extremely long conversations, with a significant proportion exceeding 60 turns and some approaching 100. This reflects the organic nature of real-world dialogues, which often involve prolonged multi-topic interactions with informal exchanges and irregular structure. The longer and noisier dialogue structure poses greater challenges for retrieval, especially in maintaining semantic consistency and aligning queries to sparse but relevant fragments.

## Appendix B: Implementation Details

### B1. Training and Hyperparameter Settings

We implement F<sup>2</sup>RVLM using the ms-swift (Zhao et al. 2024) framework, with Qwen-VL-Instruct as the backbone in 2B, 3B, and 7B configurations. Fine-tuning is conducted on the MLDR dataset, with 1,000 samples reserved for validation and the remaining for training. Among the training

data, 25% is used for SFT cold start, while the remaining is reserved for RFT. We adopt LoRA (Hu et al. 2022) for parameter-efficient adaptation during both the SFT and RFT stages. During GRPO fine-tuning in RFT, we sample  $G = 8$  candidate responses for each instance. The reward weights are set to  $\lambda_{\text{utt}} = \lambda_{\text{img}} = 0.5$ , and the exponential length penalty base is  $\gamma = 0.95$ . Curriculum sampling begins with 10% of the easy and medium-level instances and gradually incorporates confusing and hard instances as training progresses. To enhance training stability and efficiency, we adopt the dynamic sampling strategy from DAPO (Yu et al. 2025). Gradient checkpointing and FlashAttention are utilized to enhance training efficiency. All models are trained for 1 epoch on 8×A100 GPUs.

### B2. Model Comparison Settings

We evaluate F<sup>2</sup>RVLM against a comprehensive set of VLMs in three categories: (1) **Proprietary models**, including Claude-Sonnet-4, GPT-4o, Gemini-2.5-Flash, and Doubao-Seed-1.6, are accessed via public APIs in inference-only mode without any fine-tuning. (2) **Open-source generation-based models**, including LLaVa, Qwen-VL-series, DeepSeek-VL2-series, InternVL3-series, Ovis2, Owl3, and MiMo-VL, are built from official checkpoints and fine-tuned on the MLDR dataset via SFT. All SFT models adopt the same prompt template as F<sup>2</sup>RVLM and are trained in the ms-swift framework with LoRA for parameter-efficient adaptation. They share the same training configuration as F<sup>2</sup>RVLM’s SFT stage, except that all training data are used for SFT and models are trained for one epoch. (3) **Embedding-based models**, including CLIP, BLIP-2, E5-V, and GME, are evaluated in inference-only mode. We compute the embedding of the query and each utterance/image in the dialogue, then apply a similarity threshold to retrieve relevant fragments, reporting the best results across all thresholds.

### B3. Sliding Window Inference for Long Contexts

Some open-source generation-based models (e.g., Ovis2-2B, LLaVA-1.5-7B, and InternVL3-series) are constrained by limited context length and cannot directly process long-form dialogues in a single pass. To address this limitation, we adopt a sliding window inference strategy during evaluation. Specifically, the dialogue is segmented into overlapping windows of 35 turns, with an overlap of 15 turns between adjacent windows. Each window is independently processed by the model, and the fragment-level predictions are collected. For overlapping segments, we take the union of predicted results across windows to ensure comprehensive coverage and mitigate boundary truncation effects. This approach enables fair evaluation of models with limited context capacity while maintaining retrieval completeness.

## Appendix C: Experimental Results and Analysis

### C1. Detailed Comparison of Quantitative Results

Due to space limitations in the main text, Table 2 only presents the overall performance of selected models on the

Model	Utterance Retrieval				Image Retrieval				Joint Retrieval			
	Precision	Recall	F1	MCC	Precision	Recall	F1	MCC	Precision	Recall	F1	MCC
CLIP-Embedding <sup>†</sup>	45.21	20.42	28.13	12.18	52.86	62.63	57.33	30.11	48.74	30.80	42.73	21.14
BLIP2-Embedding <sup>†</sup>	30.54	78.97	44.05	0.00	33.33	1.51	2.89	0.00	31.88	2.96	23.47	0.00
E5-V-Embedding <sup>†</sup>	54.39	40.16	46.21	27.31	53.32	62.25	57.44	30.54	53.85	48.83	51.82	28.92
GME-Embedding <sup>†</sup>	56.96	33.09	41.86	26.09	68.66	18.52	29.18	22.25	62.27	23.75	35.52	24.17
Qwen2.5-VL-7B <sup>†</sup>	23.29	3.08	5.45	0.00	19.46	6.95	10.24	0.00	21.20	4.27	7.84	0.00
MiMo-7B-RL <sup>†</sup>	70.18	46.23	55.74	42.74	65.35	68.44	66.86	48.30	67.68	55.19	61.30	45.52
Qwen2.5-VL-72B <sup>†</sup>	62.42	60.67	61.54	44.27	59.85	75.15	66.63	44.95	61.11	67.14	64.09	44.61
Doubaod-Seed-1.6 <sup>†</sup>	79.69	33.69	47.36	40.79	68.78	56.42	61.99	44.36	73.83	42.19	54.67	42.57
Claude-Sonnet-4 <sup>†</sup>	69.88	48.51	57.26	43.83	64.74	72.37	68.34	49.31	67.21	58.09	62.80	46.57
GPT-4o <sup>†</sup>	73.90	46.51	57.09	46.11	67.28	60.24	63.56	45.70	70.43	52.49	60.32	45.91
Gemini-2.5-Flash <sup>†</sup>	68.85	64.85	66.79	52.27	71.56	74.42	72.96	57.06	70.18	69.30	69.87	54.66
InternVL3-1B	62.49	89.16	73.48	60.64	72.45	90.63	80.53	68.65	67.10	89.89	77.00	64.64
InternVL3-2B	72.68	91.31	80.94	71.84	79.04	92.41	85.20	76.38	75.73	91.86	83.07	74.11
Ovis2-2B	73.85	46.27	56.90	45.33	80.37	39.26	52.75	42.63	76.97	42.48	54.82	43.98
mPLUG-Owl3-2B	71.70	81.80	76.42	64.93	78.32	84.60	81.34	70.25	74.86	83.18	78.88	67.59
Qwen2-VL-2B	71.88	92.66	80.96	71.97	78.35	93.32	85.18	76.38	74.97	92.99	83.07	74.18
Qwen2.5-VL-3B	77.21	91.22	83.64	75.85	83.75	91.60	87.50	80.12	80.35	91.41	85.57	77.98
DeepSeek-VL2-Tiny-3B	58.54	83.69	68.89	52.87	68.12	84.81	75.56	60.30	62.97	84.25	72.23	56.59
<b>F<sup>2</sup>RVLM-Qwen2-VL-2B</b>	<b>76.84</b>	<b>88.86</b>	<b>82.42</b>	<b>73.97</b>	<b>82.64</b>	<b>90.25</b>	<b>86.28</b>	<b>78.16</b>	<b>79.64</b>	<b>89.55</b>	<b>84.35</b>	<b>76.07</b>
<b>F<sup>2</sup>RVLM-Qwen2.5-VL-3B</b>	<b>80.71</b>	<b>90.49</b>	<b>85.32</b>	<b>78.35</b>	<b>84.88</b>	<b>92.84</b>	<b>88.68</b>	<b>82.03</b>	<b>82.74</b>	<b>91.65</b>	<b>87.00</b>	<b>80.19</b>
LLaVa-1.5-7B-hf	63.99	91.93	75.46	63.72	72.88	92.19	81.41	70.18	68.15	92.06	78.43	66.95
MiMo-7B-SFT	79.01	92.55	85.25	78.28	84.38	93.97	88.92	82.41	81.61	93.25	87.08	80.35
MiMo-7B-RL	78.17	<b>92.85</b>	84.88	77.75	83.63	<b>94.08</b>	88.55	81.81	80.90	<b>93.46</b>	86.71	79.78
Qwen2-VL-7B	80.60	89.60	84.86	77.66	85.86	91.87	88.76	82.18	83.15	90.72	86.81	79.92
Qwen2.5-VL-7B	78.74	90.88	84.37	76.93	84.51	91.98	88.09	81.07	81.52	91.42	86.23	79.00
InternVL3-8B	77.74	92.48	84.47	77.14	83.82	93.48	88.39	81.56	80.67	92.98	86.43	79.35
DeepSeek-VL2-Small-16B	74.93	90.56	82.01	73.40	80.29	91.71	85.62	77.05	77.52	91.13	83.82	75.23
<b>F<sup>2</sup>RVLM-Qwen2-VL-7B</b>	<b>82.19</b>	<b>88.99</b>	<b>85.46</b>	<b>78.58</b>	<b>85.93</b>	<b>92.41</b>	<b>89.05</b>	<b>82.63</b>	<b>84.02</b>	<b>90.67</b>	<b>87.25</b>	<b>80.60</b>
<b>F<sup>2</sup>RVLM-Qwen2.5-VL-7B</b>	<b>81.64</b>	<b>90.49</b>	<b>85.84</b>	<b>79.12</b>	<b>84.91</b>	<b>92.73</b>	<b>88.65</b>	<b>81.97</b>	<b>83.24</b>	<b>91.60</b>	<b>87.24</b>	<b>80.55</b>

Table 6: Comparison with popular VLMs on the MLDR validation set. We report Precision, Recall, F1, and MCC for utterance, image, and joint predictions. “†” indicates zero-shot inference without MLDR fine-tuning.

MLDR and WeChat datasets in terms of joint precision, recall, F1, and MCC. To provide a more comprehensive evaluation, this section reports the full set of metrics, including separate results for utterance-level, image-level, and joint fragment-level retrieval across all models. Each category includes precision, recall, F1, and MCC, offering a finer-grained comparison of model capabilities.

**MLDR Validation Set.** Table 6 presents the comparison results on the MLDR validation set, embedding-based models (e.g., CLIP, BLIP-2, E5-V, GME) generally underperform across all metrics. Without task-specific supervision, they struggle to align utterance and image semantics, resulting in imbalanced retrieval (e.g., BLIP-2 shows extremely high utterance recall but almost zero image recall and MCC). Proprietary models (e.g., Claude, GPT-4o, Gemini, Doubaod) exhibit moderate performance, achieving reasonable F1 and MCC scores in joint retrieval, but their recall remains limited due to the lack of task adaptation. In contrast, open-source models fine-tuned with SFT on MLDR (e.g., Qwen2.5-VL, InternVL3, Owl3) demonstrate substantial improvements, balancing precision and recall and achieving higher MCC scores. Our proposed F<sup>2</sup>RVLM series outperforms all baselines in nearly all metrics. Notably, F<sup>2</sup>RVLM-7B achieves the best joint F1 (87.25%) and MCC (80.60%), and maintains strong utterance and image-level performance. Even the lighter-weight 2B and 3B variants surpass larger models such as MiMo-7B and InternVL3-8B, highlighting the ef-

fectiveness of GRPO-based fine-tuning and difficulty-aware curriculum sampling in improving fine-grained retrieval accuracy.

**WeChat Test Set.** Table 7 further evaluates the generalization performance of all models on the WeChat test set, which features longer contexts, more linguistic noise, and broader domain shifts, posing a more challenging evaluation scenario. Results show that fine-tuning on MLDR significantly improves cross-domain fragment retrieval. For instance, Qwen2.5-VL-7B improves its joint F1 from 12.58% (MCC = 0.00%) in zero-shot to 51.71% (MCC = 43.65%) after SFT on MLDR, over a fourfold increase. MiMo-7B also benefits notably from task-specific fine-tuning. These findings confirm that MLDR supervision enhances not only in-domain performance but also out-of-domain alignment and reasoning. In contrast, proprietary models such as GPT-4o and Gemini-2.5, without access to MLDR fine-tuning, still exhibit strong performance due to their massive scale and diverse pretraining corpora. Nevertheless, F<sup>2</sup>RVLM maintains consistently strong results across all model sizes. The 7B variant achieves the best joint F1 (62.07%) and MCC (55.46%), while even the lightweight 2B and 3B variants outperform larger baselines. This underscores the effectiveness of our GRPO-based optimization and curriculum-guided training in enhancing fine-grained semantic alignment and context reasoning under domain shifts.

Model	Utterance Retrieval				Image Retrieval				Joint Retrieval			
	Precision	Recall	F1	MCC	Precision	Recall	F1	MCC	Precision	Recall	F1	MCC
CLIP-Embedding <sup>†</sup>	16.44	35.99	22.57	9.15	27.01	81.37	40.55	26.08	20.44	49.91	31.56	17.62
BLIP2-Embedding <sup>†</sup>	11.00	71.41	19.07	0.00	24.68	41.81	31.04	11.97	15.22	52.74	25.05	4.94
E5-V-Embedding <sup>†</sup>	34.73	35.82	35.27	26.80	26.92	68.89	38.72	22.00	30.33	47.13	36.99	24.40
GME-Embedding <sup>†</sup>	32.54	39.12	35.52	26.51	27.19	82.67	40.93	26.86	29.63	53.11	38.22	26.68
Qwen2.5-VL-7B <sup>†</sup>	13.95	11.38	12.53	2.77	8.07	28.98	12.62	0.00	10.22	16.34	12.58	0.00
MiMo-7B-RL <sup>†</sup>	41.63	22.70	29.38	24.49	41.85	26.55	32.49	22.88	41.74	24.48	30.94	23.68
Qwen2.5-VL-72B <sup>†</sup>	28.25	27.90	28.07	18.88	38.41	54.70	45.13	31.63	32.55	36.95	36.60	25.26
Doubaod-Seed-1.6 <sup>†</sup>	61.83	21.81	32.24	32.49	49.89	41.01	45.02	35.62	55.22	28.47	38.63	34.06
Claude-Sonnet-4 <sup>†</sup>	60.38	29.89	39.98	37.69	44.36	64.68	52.63	43.31	51.15	40.88	46.30	40.50
GPT-4o <sup>†</sup>	60.43	32.19	42.01	39.18	52.37	59.65	55.77	46.52	56.11	41.82	48.89	42.85
Gemini-2.5-Flash <sup>†</sup>	48.65	36.86	41.94	35.92	55.60	76.76	64.49	<b>60.52</b>	51.89	49.80	53.21	48.22
InternVL3-1B <sup>*</sup>	19.97	<b>86.85</b>	32.48	15.27	29.69	<b>73.92</b>	42.37	41.39	23.88	<b>79.86</b>	37.42	28.33
InternVL3-2B <sup>*</sup>	28.34	81.31	42.02	22.41	35.70	67.18	46.62	44.27	31.59	73.57	44.32	33.34
Ovis2-2B <sup>*</sup>	39.72	56.87	46.77	23.54	42.00	52.34	46.60	42.79	40.83	54.51	46.69	33.16
mPLUG-Owl3-2B	20.65	45.01	28.31	16.78	16.51	47.01	24.44	6.44	18.35	45.99	26.37	11.61
Qwen2-VL-2B	18.38	86.49	30.32	23.64	31.46	67.83	42.98	29.45	23.20	76.03	36.65	26.55
Qwen2.5-VL-3B	27.77	79.03	41.11	35.70	43.02	72.86	54.09	43.41	33.75	75.82	47.60	39.56
DeepSeek-VL2-Tiny-3B	21.95	27.96	24.59	13.69	46.52	16.97	24.87	19.89	29.83	21.12	24.73	16.79
<b>F<sup>2</sup>RVLM-Qwen2-VL-2B</b>	20.99	82.21	33.45	27.11	37.72	64.04	47.48	34.70	26.97	72.00	40.46	30.90
<b>F<sup>2</sup>RVLM-Qwen2.5-VL-3B</b>	39.54	71.98	51.04	45.31	52.87	69.78	60.16	50.88	45.24	70.86	55.60	48.09
LLaVA-1.5-7B-hf <sup>*</sup>	18.16	<b>89.80</b>	30.21	9.78	24.66	<b>74.21</b>	37.02	36.20	20.91	<b>81.27</b>	33.61	22.99
MiMo-7B-SFT	40.06	52.03	45.27	37.60	<b>63.55</b>	42.16	50.69	43.82	49.14	46.58	47.98	40.71
MiMo-7B-RL	40.05	53.53	45.82	38.23	<b>64.66</b>	43.87	52.28	45.46	49.46	48.22	49.05	41.84
Qwen2-VL-7B	36.28	71.65	48.17	42.20	52.17	67.65	58.91	49.30	42.80	69.60	53.54	45.75
Qwen2.5-VL-7B	34.74	71.70	46.80	40.74	47.11	70.90	56.61	46.57	39.99	71.30	51.71	43.65
InternVL3-8B <sup>*</sup>	31.05	80.78	44.86	25.98	37.76	70.90	49.28	47.33	34.08	75.52	47.07	36.65
DeepSeek-VL2-Small-16B	40.13	24.92	30.75	24.93	57.98	16.00	25.07	24.09	47.43	19.48	27.91	24.51
<b>F<sup>2</sup>RVLM-Qwen2-VL-7B</b>	<b>52.36</b>	67.51	<b>58.98</b>	<b>53.50</b>	63.05	67.42	<b>65.16</b>	<b>57.41</b>	<b>57.21</b>	67.46	<b>62.07</b>	<b>55.46</b>
<b>F<sup>2</sup>RVLM-Qwen2.5-VL-7B</b>	<b>52.44</b>	64.51	<b>57.85</b>	52.16	57.46	65.82	61.36	52.63	54.83	65.16	<b>59.60</b>	52.39

Table 7: Comparison with popular VLMs on the WeChat test set. We report Precision, Recall, F1, and MCC for utterance, image, and joint predictions. “†” indicates zero-shot inference without MLDR fine-tuning. “\*” indicates models limited by context length, evaluated via sliding-window inference.

## C2. Comparison of Qualitative Results

We provide qualitative comparisons on the MLDR validation set (Fig.10), our F<sup>2</sup>RVLM accurately retrieves semantically complete and coherent fragments that align well with human annotations. It outperforms closed-source or open-source large models that often miss key utterances or include off-topic content. On the WeChat test set (Fig.11–12), our model demonstrates better robustness in informal, multi-topic dialogues. While closed-source and open-source models tend to produce partial or noisy results, F<sup>2</sup>RVLM captures more complete, relevant, and coherent fragments, effectively combining verbal and visual cues even in complex real-world cases. These results further validate the model’s superior capability in real-world fragment-level retrieval.

## C3. Comparison of Cross-Lingual Generalization

To assess the cross-lingual robustness, we evaluate various VLMs on an English-translated version of the WeChat test set. Specifically, we randomly sample 200 dialogues from the original set and translate each utterance into English using DeepL Translator to preserve semantic fidelity. The translated set maintains the original structure and multi-

modal content, enabling fair comparison across languages.

As depicted in Table 8, even though models like Claude-4 and GPT-4o exhibit strong zero-shot performance due to extensive pre-training on English corpora, our F<sup>2</sup>RVLM-7B achieves the highest overall joint F1 (57.49%) and MCC (50.69%). Even the 3B variant of F<sup>2</sup>RVLM outperforms larger models like MiMo-7B and Qwen2.5-VL-7B, confirming its strong generalization with fewer parameters. Importantly, unlike some VLMs that exhibit skewed retrieval behavior (e.g., high precision but low recall, or vice versa), F<sup>2</sup>RVLM achieves a more balanced trade-off between precision and recall. This balance results in consistently higher F1 and MCC scores, highlighting the model’s ability to perform fine-grained fragment retrieval across languages. The above results suggest that the reward-guided fine-tuning strategy in F<sup>2</sup>RVLM effectively transfers to different linguistic settings, supporting fine-grained fragment alignment and reasoning beyond Chinese-language contexts.

## C4. Human Subjective Evaluation Criteria

To assess the human-perceived quality of fragment-level retrieval, we randomly sample 200 dialogues and ask expert annotators to compare model outputs under identical input contexts. Each annotator is instructed to select the best-performing model according to the following three criteria:

Model	Utterance Retrieval				Image Retrieval				Joint Retrieval			
	Precision	Recall	F1	MCC	Precision	Recall	F1	MCC	Precision	Recall	F1	MCC
Qwen2.5-VL-72B <sup>†</sup>	30.31	32.04	31.15	21.57	34.23	73.56	46.72	36.60	32.15	44.64	38.94	29.08
Claude-4 <sup>†</sup>	59.09	39.46	47.32	42.82	59.05	59.62	59.33	51.83	59.07	47.49	53.32	47.32
GPT-4o <sup>†</sup>	64.18	34.54	44.91	42.23	53.69	62.98	57.96	49.74	58.47	44.61	51.43	45.99
Gemini-2.5 <sup>†</sup>	59.94	26.56	36.81	35.00	52.25	47.21	49.60	41.13	55.83	33.99	43.20	38.06
mPLUG-Owl3-2B	22.32	16.92	19.25	10.14	16.71	29.81	21.42	5.13	19.11	21.59	20.33	7.64
Qwen2-VL-2B	15.90	86.34	26.86	16.69	27.57	81.25	41.17	30.58	20.17	83.72	34.01	23.64
Qwen2.5-VL-3B	23.78	76.42	36.27	28.87	34.47	72.60	46.75	36.50	28.15	74.46	41.51	32.68
Mimo-7B-RL	37.44	40.92	39.10	30.49	64.75	37.98	47.88	43.04	47.44	39.39	43.49	36.77
Qwen2-VL-7B	38.85	56.66	46.09	38.14	47.47	58.65	52.47	43.00	42.73	57.64	49.28	40.57
Qwen2.5-VL-7B	34.82	63.52	44.98	37.27	44.90	67.79	54.02	44.91	39.22	65.59	49.50	41.09
DeepSeek-VL2-Small-16B	26.43	14.66	18.86	11.97	55.88	9.69	16.52	18.72	35.89	11.67	17.69	15.35
<b>F<sup>2</sup>RVLM-Qwen2-VL-2B</b>	17.03	86.27	28.45	19.51	29.80	78.37	43.18	32.78	21.68	82.13	35.81	26.14
<b>F<sup>2</sup>RVLM-Qwen2.5-VL-3B</b>	30.25	70.18	42.28	35.00	42.11	73.08	53.43	44.60	35.21	71.60	47.85	39.80
<b>F<sup>2</sup>RVLM-Qwen2-VL-7B</b>	50.19	53.81	51.94	45.23	62.15	63.94	63.03	56.15	55.54	58.44	57.49	50.69

Table 8: Evaluation results on the English-translated WeChat test set. We report precision, recall, F1, and MCC for utterance, image, and joint retrieval. “<sup>†</sup>” indicates zero-shot inference without MLDR fine-tuning.



Figure 10: Qualitative comparison on the MLDR validation set. Given a user query, we visualize one representative case of retrieved fragments from various models. Pre-trained models often retrieve semantically relevant but incomplete or disjointed fragments. MLDR fine-tuned models improve alignment but may still miss contextual boundaries. Our F<sup>2</sup>RVLM-7B achieves the most coherent and complete retrieval, accurately aligning both utterances and images with the intended semantics.

- **Coverage**, which measures whether the retrieved fragment fully captures all key information relevant to the user query. It emphasizes completeness, particularly the inclusion of essential contextual elements. Fragments that contain more content can still receive high coverage scores as long as they thoroughly address the query without omitting important details.
- **Relevance**, which evaluates how well the retrieved content semantically aligns with the user query. Every utterance and image in the fragment should directly relate to the query’s core intent. Even if some parts are on-topic, the presence of off-topic or irrelevant content will reduce the relevance score.

- **Coherence**, which assesses the logical flow and clarity of the retrieved fragment itself. It focuses on whether the sentences and images are naturally connected, well-organized, and easy to understand when read as a self-contained unit. This evaluation does not consider the broader dialogue context, but strictly the internal consistency of the retrieved segment.

If multiple models produce identical and top-performing outputs for a given dialogue, annotators will select all such models. As a result, the total number of top-choice selections may exceed the number of dialogues evaluated.



Figure 11: Case 1 of qualitative comparison on the WeChat test set, focusing on a personal-life dialogue scenario.

### Query: INode 安装问题

Ground-truth:  
<|utt\_ids\_start|>[20, 21, 22, 23]<|utt\_ids\_end|>;  
<|img\_ids\_start|>[0]<|img\_ids\_end|>

Claude-Sonnet-4—Pre-trained Only:  
<|utt\_ids\_start|>[20, 21, 22, 23]<|utt\_ids\_end|>;  
<|img\_ids\_start|>[0]<|img\_ids\_end|>

Gemini-2.5-Flash—Pre-trained Only:  
<|utt\_ids\_start|>[20, 21, 23]<|utt\_ids\_end|>;  
<|img\_ids\_start|>[0]<|img\_ids\_end|>

Douba-Seed-1.6—Pre-trained Only:  
<|utt\_ids\_start|>[20, 21, 23]<|utt\_ids\_end|>;  
<|img\_ids\_start|>[0, 2]<|img\_ids\_end|>

Qwen2.5-VL-72B—Pre-trained Only:  
<|utt\_ids\_start|>[20, 21, 23, 36, 37]<|utt\_ids\_end|>;  
<|img\_ids\_start|>[2]<|img\_ids\_end|>

MiMo-7B-RL—MLDR Fine-tuned:  
<|utt\_ids\_start|>[20, 21, 22, 23, 24, 39]<|utt\_ids\_end|>;  
<|img\_ids\_start|>[0, 2]<|img\_ids\_end|>

Qwen2.5-VL-7B—MLDR Fine-tuned:  
<|utt\_ids\_start|>[20, 21, 22, 23, 24, 37, 38, 39, 40]<|utt\_ids\_end|>;  
<|img\_ids\_start|>[0, 2, 3]<|img\_ids\_end|>

Our F2VLM-7B—MLDR Fine-tuned:  
<|utt\_ids\_start|>[20, 21, 22, 23]<|utt\_ids\_end|>;  
<|img\_ids\_start|>[0]<|img\_ids\_end|>

utt\_id0: 师弟，我是博二的师弟，最近准备撰写论文，老师说您有投`paper`的经验，建议我和您聊一聊，敢取经，师兄您今天下午不方便呀

utt\_id1: 可以啊，还是太猛了

utt\_id2: 没有没有，之前没写论文的经验，还是得和师兄多请教，下午几点方便呀

utt\_id3: 行啊，我下午应该在所里，3点？

utt\_id4: 好的师兄，您会在哪呢？

utt\_id5: 师兄，不好意思，刚从医院出来，被叫出来开会了。我记得您住在605号，我晚上回宿舍来找你！

utt\_id6: 好的师兄，没问题，我在605号

utt\_id7: 好的，我晚上到宿舍跟你说话。

utt\_id8: 晚上快到宿舍提前十分钟左右跟我说，我回宿舍。

utt\_id9: 好的，没事师弟，不用这么客气。

utt\_id10: 好嘞师兄。

utt\_id11: 师弟我回来了，你在宿舍么

utt\_id12: 师兄，明天你在那里嘛？要不咱俩明天白天找找个时间，现在有些太晚了，也影响师兄休息。

utt\_id13: 行啊师哥，不好意思，回来太晚了，明天我在所里。到时候我找师弟聊。嗯，师弟早点休息。

utt\_id14: 哼嘿，师兄也早点休息。

utt\_id15: 师弟你在那里嘛？

utt\_id16: 对，师兄，我去找你吧。

utt\_id17: 稍等哈，我5分钟到所里。

utt\_id18: 好的，师兄，要不咱们去一楼？

utt\_id19: 我到了。你来我办公室吧。我屋子没人。

utt\_id20: 师兄，INode安装包发一下。

utt\_id21: 这是当时师兄给我的，师兄你试试。

[https://1drv.ms/u/s!Ap\\_l6gYcFgSVz3UPYg6tOxL7B?e=7RwQJ](https://1drv.ms/u/s!Ap_l6gYcFgSVz3UPYg6tOxL7B?e=7RwQJ)



utt\_id22: 哟嘿对，还是上次那个位置，应该就在工位上，你拍一下吧。

utt\_id23: 呀对。是这两个。都要给哈。

utt\_id24: 就这俩是吧。

utt\_id25: 对的。

utt\_id26: 你中午去食堂吃饭的时候帮我个忙，把我的工位上的两个三会一课的本子，给一下党支部老师。

utt\_id27: 现在去可以不可以？

utt\_id28: 可以啊。麻烦了麻烦了。

utt\_id29: 没事没事。你工位还是上次那个位置吧。

utt\_id30: 哟嘿对，还是上次那个位置。

utt\_id31: 哟嘿对，还是上次那个位置。

utt\_id32: 就这俩是吧。

utt\_id33: 好的。

utt\_id34: 好的。

utt\_id35: 万分感谢师兄，改天找你吃饭。

utt\_id36: 客气师兄。

utt\_id37: 应该是1318进去，桌子上有三会一课本子的那个位置。麻烦啦~。

utt\_id38: 好的。

utt\_id39: 放这里了。

utt\_id40: 好滴拿师弟。

### Query: INode 安装问题

Ground-truth:  
<|utt\_ids\_start|>[20, 21, 22, 23]<|utt\_ids\_end|>;  
<|img\_ids\_start|>[0]<|img\_ids\_end|>

Claude-Sonnet-4—Pre-trained Only:  
<|utt\_ids\_start|>[20, 21, 22, 23]<|utt\_ids\_end|>;  
<|img\_ids\_start|>[0]<|img\_ids\_end|>

Gemini-2.5-Flash—Pre-trained Only:  
<|utt\_ids\_start|>[20, 21, 23]<|utt\_ids\_end|>;  
<|img\_ids\_start|>[0]<|img\_ids\_end|>

Douba-Seed-1.6—Pre-trained Only:  
<|utt\_ids\_start|>[20, 21, 23]<|utt\_ids\_end|>;  
<|img\_ids\_start|>[0, 2]<|img\_ids\_end|>

Qwen2.5-VL-72B—Pre-trained Only:  
<|utt\_ids\_start|>[20, 21, 23, 36, 37]<|utt\_ids\_end|>;  
<|img\_ids\_start|>[2]<|img\_ids\_end|>

MiMo-7B-RL—MLDR Fine-tuned:  
<|utt\_ids\_start|>[20, 21, 22, 23, 24, 39]<|utt\_ids\_end|>;  
<|img\_ids\_start|>[0, 2]<|img\_ids\_end|>

Qwen2.5-VL-7B—MLDR Fine-tuned:  
<|utt\_ids\_start|>[20, 21, 22, 23, 24, 37, 38, 39, 40]<|utt\_ids\_end|>;  
<|img\_ids\_start|>[0, 2, 3]<|img\_ids\_end|>

Our F2VLM-7B—MLDR Fine-tuned:  
<|utt\_ids\_start|>[20, 21, 22, 23]<|utt\_ids\_end|>;  
<|img\_ids\_start|>[0]<|img\_ids\_end|>

utt\_id0: 师弟，从`far1m`数据集里面找100张图，这100张图里面要包含`far1m`里面的五个大类，只需要找出米图片就行。数据下载地址：[https://blog.csdn.net/ferry\\_Jack/article/details/120673622](https://blog.csdn.net/ferry_Jack/article/details/120673622)，争取周末放假前整理完给我。

utt\_id1: 好的，师弟，我帮您找一下。

utt\_id2: 图片里面有五个大类，你找出来的这100张图也包含这五个大类就行。

utt\_id3: 收到，是这周六之前吗。

utt\_id4: 对的。

utt\_id5: 师兄，这是总共100张图片，每张图片都包含这五个大类，具体是五大类内嵌的哪一大类没有关系。

utt\_id6: 不用每张图片，100张图里面总共包含5大类就行，内部的分类无关紧要。

utt\_id7: 哦，好滴。师兄，这个是我整理好的图片和对应的label。相对的类别还有两个分类的图片都保存在excel里了。

utt\_id8: 好的师弟，辛苦了。

utt\_id9: 师弟最近有时间吗？

utt\_id10: 师兄，这两天家里有点事情，过两天再说。

utt\_id11: 好的，那你先忙。

utt\_id12: 有什么任务吗？我可以抽空先带起来。

utt\_id13: 帮一下数据，标注公司的数据反馈回来了，需要整理一下。

utt\_id14: 哟嘿。师兄，像这种`bottom`的意思是在另外一个飞机的下面，不是指在图片的下面。



utt\_id22: 还好，是有什么事情吗？

utt\_id23: 麻烦师弟把2D框标注和文本框描述统计一下，统计`cap`字段按30775。

utt\_id24: 好的师兄，这就算一个2D框一个描述，对吗？



utt\_id25: 对的。

utt\_id26: 好的。

utt\_id27: 师弟，按`cap`字段来统计，`cap`出现的次数就是标注的数量，麻烦师弟重新统计一下。



utt\_id28: 我现在在外面，手头没电脑，晚上搞可以吗？

utt\_id29: OK不着急。

utt\_id30: 师兄，我现在要改的是2D框的数量还是描述的数量啊，我还是不太明白。

utt\_id31: `cap`的数量，有一定的出入。师弟和公公司的统计都有出入，你统计`cap`字段是30775吗。

utt\_id32: 我统计到30754。

utt\_id33: 阿这，问题不大，那就30755吧。

utt\_id34: 好的。

Query: 标注和文本框描述统计

Ground-truth:  
<|utt\_ids\_start|>[23, 24, 25, 26, 27, 28, 29, 30, 31, 32, 33]<|utt\_ids\_end|>;  
<|img\_ids\_start|>[3]<|img\_ids\_end|>

Claude-Sonnet-4—Pre-trained Only:  
<|utt\_ids\_start|>[27, 31, 32]<|utt\_ids\_end|>;  
<|img\_ids\_start|>[]<|img\_ids\_end|>

Gemini-2.5-Flash—Pre-trained Only:  
<|utt\_ids\_start|>[23, 27, 30, 31, 32, 33]<|utt\_ids\_end|>;  
<|img\_ids\_start|>[3]<|img\_ids\_end|>

Douba-Seed-1.6—Pre-trained Only:  
<|utt\_ids\_start|>[]<|utt\_ids\_end|>;  
<|img\_ids\_start|>[]<|img\_ids\_end|>

Qwen2.5-VL-72B—Pre-trained Only:  
<|utt\_ids\_start|>[31]<|utt\_ids\_end|>;  
<|img\_ids\_start|>[]<|img\_ids\_end|>

MiMo-7B-RL—MLDR Fine-tuned:  
<|utt\_ids\_start|>[27, 28, 29, 30, 31, 32, 33]<|utt\_ids\_end|>;  
<|img\_ids\_start|>[]<|img\_ids\_end|>

Qwen2.5-VL-7B—MLDR Fine-tuned:  
<|utt\_ids\_start|>[27, 28, 29, 30, 31, 32, 33]<|utt\_ids\_end|>;  
<|img\_ids\_start|>[]<|img\_ids\_end|>

Our F2VLM-7B—MLDR Fine-tuned:  
<|utt\_ids\_start|>[23, 24, 25, 26, 27, 28, 29, 30, 31, 32, 33]<|utt\_ids\_end|>;  
<|img\_ids\_start|>[3]<|img\_ids\_end|>

Figure 12: Case 2 of qualitative comparison on the WeChat test set, illustrating fragment retrieval in a technical-support dialogue scenario.

### C5. Ablation Studies on SFT and GRPO Ratio

Table 9 explores the impact of different proportions of SFT and GRPO-based RFT on model performance. We observe the following: (1) Using GRPO alone underperforms compared to using only SFT, highlighting the indispensable role

of supervised learning for cold-start in providing stable and accurate training signals; (2) As the proportion of GRPO increases, overall performance gradually surpasses that of pure SFT, demonstrating the effectiveness of RFT for dialogue fragment retrieval; (3) A 25% SFT and 75% GRPO

Training Strategy	In-domain		Real-domain	
	F1(%)	MCC(%)	F1(%)	MCC(%)
All SFT	85.57	77.98	47.60	39.56
All GRPO(0.1% SFT)	82.14	73.29	45.47	37.81
5%SFT+95%GRPO	84.58	78.65	53.64	42.83
10%SFT+90%GRPO	86.44	79.26	54.51	47.18
25%SFT+75%GRPO	87.00	80.19	<b>55.60</b>	<b>48.09</b>
50%SFT+50%GRPO	<b>87.37</b>	<b>81.05</b>	54.32	47.33

Table 9: Ablation study of different SFT and GRPO data ratios in F<sup>2</sup>RVLM on MLDR validation and WeChat test sets.

ratio achieves the best results on the real-domain test set, while increasing SFT to 50% slightly improves in-domain validation performance but compromises generalization to real-world scenarios.